universität wien

MASTERARBEIT / MASTER'S THESIS

Titel der Masterarbeit / Title of the Master's Thesis

Effects of conformational differences in anti-MOG antibodies on experimental encephalomyelitis

verfasst von / submitted by

Lucas Rohr, B.Sc.

angestrebter akademischer Grad / in partial fulfilment of the requirements for the degree of

Master of Science (MSc)

Wien, 2021/ Vienna, 2021

Studienkennzahl lt. Studienblatt / degree programme code as it appears on the student record sheet:	UA 066 834
Studienrichtung lt. Studienblatt / degree programme as it appears on the student record sheet:	Masterstudium Molekulare Biologie
Betreut von / Supervisor:	ao. Univ.-Prof. Dr. Jan Bauer

Acknowledgment

First and foremost, I want to thank my supervisor Jan Bauer as well as Ulrike Köck for their continued support throughout the process that led to this thesis. I learned a lot at the Department of Neuroimmunology at the Center for Brain Research and I thank everyone who helped me there. I especially want to thank Katharina Mair as well; our collaboration was an important part of my thesis and I could not have done it without her.

Abstrakt

Die Ursache für demyelinisierende Krankheiten wie Multiple Sklerose und Myelin-Oligodendrozyten-Glykoprotein-Antikörper-assoziierte Krankheit entzieht sich noch heute der Wissenschaftsgemeinde. Wenn wir den autoimmunen Aspekt dieser Krankheiten betrachten, wurde insbesondere die Rolle von Lymphozyten ausgiebig erforscht, doch Autoantikörper und ihre Glykosylierungsmuster sind nun auch immer mehr in den Vordergrund gerückt. Bisherige Studien haben gezeigt, dass Afukosylierung von Antikörpern zu erhöhter Affinität für FcγRIIIα geführt hat, welches in großen Mengen an der Oberfläche von natürlichen Killer (NK)-Zellen exprimiert wird, was eine Verbindung zwischen demyelinisierenden Krankheiten, welche mit erhöhter Antikörperafukosylierung einhergehen, und erhöhter antikörperabhängiger zellulärer Zytotoxizität im zentralen Nervensystem bedeuten könnte. In dieser Masterarbeit wurde als Modell experimentelle autoimmune Enzephalomyelitis aktiv mit Myelin-Oligodendrozyten-Glykoprotein in C57BL/6-Mäusen induziert. Es wurde untersucht, ob intravenöse Injektion von autoantigenem Immunoglobulin G_1 mit erhöhter Afukosylierungsrate Einfluss auf klinische Parameter (Clinical Score, Überleben, Genesung) sowie Neuropathologie (veranschaulicht durch histochemischen und immunhistochemischen Färbungen) im Rückenmark von Tieren, die an unterschiedlichen Zeitpunkten geopfert wurden, nimmt. Wir konnte zeigen, dass IgG_1-Afukosylierung Krankheitsverlauf und Überlebensrate verschlechterte und Genesung hinderte. Injektion erhöhte auch das Ausmaß der Demyelinisierung und die Zahl der perivaskulären Entzündungen im Rückenmark ohne die Zahl an B-Zellen, T-Zellen, $CD161c^+$ NK-Zellen oder $CD161c^+$ natürlichen Killer T (NKT)-Zellen im Parenchym oder perviaskulären Raum zu beeinflussen. Trotz des Zusammenhanges zwischen Antikörperfukosylie-rung und NK-Zellrekrutierung, könnten vorrangig andere Kompartimente des Immunsystems für die Änderungen in Krankheitsverlauf und Neuropathologie verantwortlich sein.

Abstract

The cause for demyelinating diseases such as multiple sclerosis and myelin oligodendrocyte glycoprotein (MOG) antibody-associated disease still eludes the scientific community to this day. When looking at the autoimmune aspect of these diseases, much emphasis has been put on investigating the role of lymphocytes, but autoantibodies and their glycosylation patterns have become a point of increasing interest as well. Previous studies have shown that afucosylation of antibodies increases their affinity for FcγRIIIα prominently expressed on the surfaces of natural killer (NK) cells which could mean a connection between demyelinating diseases associated with increase in antibody afucosylation and antibody-dependent cellular cytoxicity (ADCC) in the CNS. Using C57BL/6 mice with experimental autoimmune encephalomyelitis (EAE) actively induced with MOG as a model, this thesis investigates whether intravenous injection of auto-antigenic immunoglobulin G_1 with increased afucosylation rate affects clinical parameters (clinical scoring, survival, recovery) and/or neuropathology (visualized by histochemical and immunohistochemical stains) within the spinal cords of animals sacrificed at different time points. We were able to show that IgG_1 afucosylation exacerbated disease course, decreased survivability, and hindered recovery. Injection also increased the extent of demyelination and the number of perivascular cuffs around blood vessels within the spinal cord white matter without affecting B cell, T cell, $CD161c^+$ NK cell, or $CD161c^+$ natural killer T (NKT) cell counts in the parenchyma and perivascular space. Despite the association of antibody afucosylation with NK cell recruitment, other compartments of the immune system might be primarily responsible for changes to disease course and neuropathology.

Contents

Part I

Introduction

Chapter 1

Experimental autoimmune encephalomyelitis (EAE)

Experimental autoimmune encephalomyelitis (EAE) is an inflammatory, neurodegenerative disorder involving $CD4^+$ helper T lymphocyte-mediate demyelination in the central nervous system (Miller & Karpus, 2007). It is a well-established mouse model for multiple sclerosis (MS); however, due to the complexity of the pathology and progression of MS, there is no one single EAE model that can give us a holistic view of the disease. As such, various types of EAE models have been developed representing different aspects of MS. These can differ from each other in mouse strains, auto-antigen, and method of induction (Sato et al., 2018).

1.1 Induction

1.1.1 Active EAE

There are two ways to induce EAE – actively or passively by adoptive transfer of activated T cells.

> *"Active EAE consists of an induction and an effector phase."* (Miller & Karpus, 2007)

EAE is induced by subcutaneous immunization with CNS tissue or myelin peptides, such as proteolipid protein (PLP), myelin basic protein (MBP), or myelin oligodendrocyte glycoprotein (MOG) suspended in Complete Freund's adjuvant (CFA) (Stromnes & Goverman, 2006). The antigen used depends on the type of EAE required for a given study. To take two of the examples above, PLP is used to induce relapsing-remitting EAE and MOG is used to induce chronic-progressive EAE (Miller & Karpus, 2007). CFA is a suspension of desiccated bacteria – either Mycobacterium tuberculosis, or Bordetella pertussis – in mineral oils such as paraffin. The emulsion is ensured by an additional surfactant such as mannide monooleate. As an inflammatory agent it increases the humoral immune response (Hanlon & Vanderah, 2010; Schuhmacher, 2014). Inflammation may be aided even further by subsequent injections with pertussis toxin (Miller & Karpus, 2007). Consequently, the animals produce T lymphocytes targeting the corresponding peptide.

This leads into the effector phase where the activated $CD4^+$ helper T lymphocytes (Th

cells) breach the blood-brain barrier and release chemokines and cytokines as they recognize the autoantigenic peptide epitopes, causing an influx of peripheral mononuclear phagocytes into the parenchyma of the CNS and activation of both peripheral macrophages as well as microglia. The cytotoxic effect of the cytokines and the phagocytic activity result in demyelination of CNS axonal tracts (Miller & Karpus, 2007).

1.1.2 Passive EAE

Unlike in active EAE, passive EAE involves the adoptive transfer of activated myelin-specific T lymphocytes. First, analogous to active EAE, an animal is immunized with a myelin peptide and CFA, causing the production of myelin-specific T cells. These cells are then extracted, isolated, and cultured in a cell medium before being activated and transferred to a naïve host animal, inducing EAE (Mannara et al., 2012; Schuhmacher, 2014). Since the induction phase does not happen in the host animal, its potential side- and after-effects do not negatively affect the accuracy of tests tailored to investigate the effector phase of EAE. Another advantage of passive EAE is that it allows *in vitro* manipulation of the myelin-specific T cells to investigate the role of specific cytokines and other biological agents. The cells can also be labeled and tracked within the host animal – allowing insight into their migration, localization, interactions with other cell types and survival (Mannara et al., 2012). It has been shown that around 80% of T cells in early active lesions in MS are positive for CD8, rather than CD4. As such, alternative models that involve induction by $CD8^+$ T cells have also been developed in the past 20 years (Schuhmacher, 2014; Wekerle, 2008).

1.2 Symptoms & progression

In mice, onset of active EAE takes about 10-12 days, while it already occurs after 6-8 days in passive EAE. Generally, the animals will first exhibit muscle weakness in the tail and later in one or both hindlegs. As the disease progresses, this weakness devolves into severe paralysis. In the most severe stages of the disease, the mice may become quadriplegic and potentially die. Under normal circumstances surviving mice would make a partial or full recovery. However, aside from the autoantigen, progression and recovery also strongly depend on the strain of transgenic mice used. For instance, in case of MOG-EAE, mouse strains, such as PL/J (H-2u) and B10.PL (H-2u), usually make a full recovery after an acute, self-limiting course of the disease. SJL (H-2s) mice show a relapsing-remitting course of paralysis, making this strain an interesting model for the late stages of MS. A.SW mice develop a primary progressive course accompanied by plaque-like demyelination and antibody deposition in the absence of oligodendrocyte apoptosis; however, when paired with supplemental Bordetella pertussis, these mice show a phenotype resembling secondary progressive MS (Miller & Karpus, 2007; Sato et al., 2018).

Chapter 2

Myelin

Myelin sheaths are lipid-rich extensions of the plasma membranes of specialized cells, surrounding the axons of certain neurons in both the central and peripheral nervous system. They have an insulating and protective function. They form so-called internodes along the axon separated by short (about 1 µm), unmyelinated sections called Nodes of Ranvier. The presence of myelin significantly increases resistance to movement of charges across the cell membrane, increasing the speed at which the signal is transmitted within the axon's cytoplasm. Despite that, the voltage signal does dissipate with distance and hence must be amplified by sodium influx through voltage-gated sodium channels accumulated at the nodes of Ranvier. This type of signal transmission is called saltatory propagation of action potentials (Grider et al., 2021).

In unmyelinated neurons, the signal must run continuously along the length of the axon, both severely diminishing the velocity at which it can travel and the distance it can reach before fully dissipating (Grider et al., 2021).

2.1 Structural role of MOG in myelin of the CNS

While myelin-associated glycoprotein (MAG) is exclusively present in the periaxonal glial membrane of the myelin, serving a function in anchoring and signaling between the myelin-forming cell and the axolemma, MOG is exclusive to the exterior surface of the myelin sheath. MOG seems to have a function in transmitting information to the oligodendrocyte from the extracellular matrix or adjacent myelin sheaths; however, its role is still not well understood as MOG-null mutants seem to develop a normal phenotype (Rasband & Macklin, 2012).

2.2 Demyelination & remyelination

Especially for motor neurons, myelination is essential, as the loss of saltatory signal propagation prevents the signal – if it arrives at its destination at all – from eliciting any appropriate response in its target. Depending on the distance between origin and target, and the extent of demyelination, this causes anything from muscle weakness to complete paralysis. Such is the case in both MS and EAE (Coggan et al., 2015).

After the oligodendrocytes have been destroyed and phagocytized by the immune system and inflammation recedes, oligodendrocyte progenitor cells (OPCs) differentiate into new

oligodendrocytes to replace them – regenerating the myelin – leading to remission of symptoms. However, if the cycle repeats itself several times, eventually, the pool of progenitor cells is depleted, and regeneration becomes impossible, leading to secondary-progressive MS or EAE (Penderis et al., 2003).

Chapter 3

The blood-brain barrier (BBB)

The BBB is the system that makes the CNS a so-called immune-privileged site; it controls entry of blood-borne molecules and cells into the parenchyma, maintaining a stable environment for neurons. However, the BBB is not completely impervious and should be considered a strong filter born by virtue of both cellular and acellular components (Murphy & Weaver, 2017).

3.1 Composition of the BBB

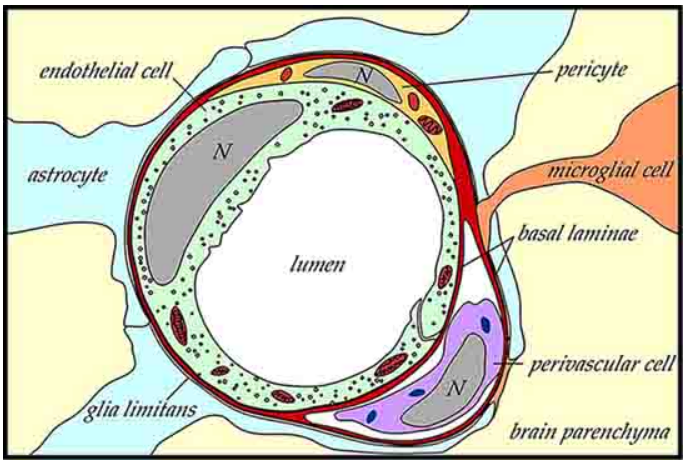

Figure 3.1: The BBB is constituted by several elements and represents a protective barrier that makes the CNS an immune-privileged site. Republished with permission of Frontiers in Bioscience, from Sawchenko, P. E. (2003). Signaling the brain in systemic inflammation the role of perivascular cells. *Frontiers in Bioscience*, 8(6), s1321–1329; permission conveyed through Copyright Clearance Center, Inc.

The BBB is primarily constituted of the endothelial cells with their basement membrane enclosing the cerebral blood vessels' lumen, the pericytes aiding in formation and maintenance of the BBB, the perivascular space, the parenchymal (glial) basement membrane, and the astrocytic end-feet involved in structural support and regulation of blood flow by means of dilation and constriction (Engelhardt & Ransohoff, 2012; Kubotera et al., 2019; El-Khoury

et al., 2006).

Unlike the endothelial cells normally found in the walls of blood vessel, the endothelial cells at the BBB do not form fenestrae, pores in the cell lining which permit the exchange of molecules, cells, extracellular fluids, and other particles (Daneman & Prat, 2015). Instead, they are strongly interconnected by adherens and tight junctions, show a greatly reduced rate of pinocytosis and high electrical resistance, and tightly regulate transport of nutrients. As such, under physiological conditions, not activated immune cells cannot pass through (Banks, 2009). The two comparably thick basement membranes delimit the perivascular space, being involved in both functioning as a barrier as well as signaling and cell adhesion (Nakato & Li, 2016).

3.1.1 Resident immune cells of the BBB

Under normal circumstances, there are three types of resident immune cells associated with the CNS: antigen-presenting cells, microglia, and surveilling lymphocytes (Ousman & Kubes, 2012). Antigen-presenting cells are found in the perivascular space, the meninges as well as the choroid plexus, even though they might vary in their makeup and ratios of subtypes. This group includes macrophages and dendritic cells (Chastain et al., 2011).

Microglia are located in the parenchyma of the CNS and represent its resident mononuclear phagocytes. Surveilling lymphocytes are predominantly located in the perivascular space with antigen-presenting cells, with a few being scattered throughout the parenchyma. (Hickey, 2001)

3.1.2 Movement of T cells across the BBB

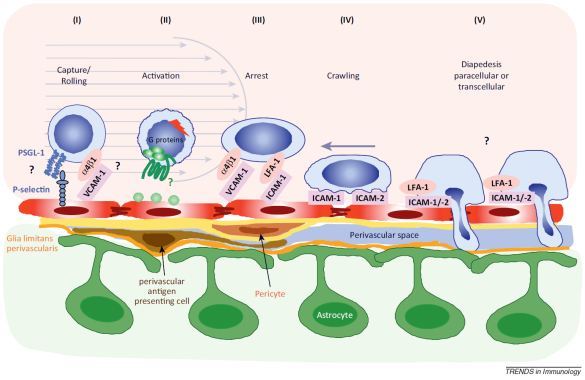

Figure 3.2: T cell migration across the endothelial basement membrane of the BBB. The inflamed endothelial cells express adhesion molecules and chemotactic factors, capturing T cells passing through the bloodstream, allowing for their subsequent activation and migration through the endothelium. Republished with permission of Elsevier, from Engelhardt, B. & Ransohoff, R. M. (2012). Capture, crawl, cross: The T cell code to breach the blood–brain barriers. *Trends in Immunology*, 33(12), 579–589; permission conveyed through Copyright Clearance Center, Inc.

While we often associate the invasion of the brain by cells of the peripheral immune system with auto-immune diseases, it is a vital mechanism whose absence would be devastating; Natalizumab is a monoclonal antibody inhibiting α4-integrins used to treat multiple sclerosis.

While Natalizumab does alleviate symptoms, it also comes with a dangerous side effect. As Natalizumab prevents T cells from passing through the BBB, they cannot errantly elicit an immune response that would damage structures in the CNS; however, this also makes the CNS increasingly susceptible to infection (Brandstadter & Katz Sand, 2017).

Given the risks associated with T cells entering the CNS, the BBB represents a checkpoint that prevents errant activation of and subsequent invasion by a given T cell; to fully cross the healthy BBB, the T cell needs to not only be activated, but also re-activated. The number of T cells that find their way into the perivascular space is low, since the endothelial cells of the resting BBB only express a limited amount of adhesion molecules on their luminal side, but a T cell that is activated in the periphery expresses adhesion ligands on its surface and can still potentially attach itself to the endothelium, passing through it via diapedesis. However, once in the perivascular space the T cell cannot penetrate into the parenchyma of the CNS unless it is re-activated by resident antigen-presenting cells. And even after entering the parenchyma the T cell requires activated microglia expressing MHC molecules to act, which does not happen often since the CNS is usually shielded from pathogens (Goverman, 2009).

Chapter 4

Inflammation in the CNS

4.1 Induction of inflammation

There are several consequences as a result of a T cell finding its specific antigen within the CNS and becoming activated. T cell-derived cytokines induce upregulation of adhesion molecules on the luminal side of endothelial cells, allowing locally confined recruitment of immune cells at the site of T cell activation. Microglia are activated as well, and – together with astrocytes – start producing chemokines such as chemokine ligand 2 (CCL2). These events lead to the formation of an inflammatory lesion (Semple et al., 2010). Inflammatory lesions are followed by entry of additional immune cells, such as non-specific T cells and macrophages, and by access to the brain for antibodies and components of the complement system (McGavern, 2005; Sevenich, 2018; Lassmann, 2020; Urich et al., 2006).

4.2 The innate immune system

The innate immune response is the first line of defense against microbes. It features both cellular and biochemical defense mechanisms and can respond rapidly to infections and products of injured cells. The mechanisms of innate immunity are relatively non-specific in their ways of dealing with different pathogens and the response to a given microbe does not change even in case of repeated infection (Abbas et al., 2018). The innate and adaptive immune system reciprocally activate each other.

4.2.1 Macrophages & microglia

Macrophages are a type of phagocytic cell with antigen-presenting capabilities, i.e., they express MHC II molecules on their surfaces, which hold the antigen in place for recognition by lymphocytes of the adaptive immune system. Microglia are the resident macrophages of the CNS, being evenly distributed within it and accounting for about 10% of its cells. Under physiological conditions – in their resting state – they show a ramified morphology and monitor their surroundings with their extended processes. When microglia recognize a disturbance, be it inflammation, infection, or damage, they retract their appendices, taking an ameboid shape, start producing surface proteins typical for macrophages, and undergo strong local proliferation. Depending on the signaling pathway they are exposed to, their priority can be

shifted towards attacking microbes or aiding in debris removal and regeneration (Goldmann & Prinz, 2013). It should be noted that microglia have the ability to synthesize both pro- and anti-inflammatory molecules – being able to act both neuroprotective by producing brain-derived neurotrophic factor (BDNF) or neurodestructive by producing reactive oxygen and nitrogen species (Gomes et al., 2013; Simpson & Oliver, 2020). Microglia also have functions outside of pathological conditions; they are involved in synapse pruning and formation as well as myelin turnover (Andoh et al., 2019; Goldmann & Prinz, 2013).

4.2.2 Dendritic cells (DCs)

DCs represent the most powerful antigen-presenting cells. Similar to microglia, they show a ramified, or rather dendritic morphology in their resting state. Since they are the most important inducers of the adaptive immune system, they are often termed sentinel cells of the immune system. This cell type is heterogenous in location, migration pathways, signal and stimuli dependence, and protein expression. They play a vital role in inducing tolerance, memory, Th cell differentiation and various other aspects of adaptive immunity (Roghanian, 2021).

Chapter 5

The adaptive immune system

The adaptive immune system mainly comprises the lymphocytes and their secreted products, including antibodies. As it encounters new foreign substances, it memorizes them as antigens, and the parts thereof which are recognized by the lymphocytes are called determinants or epitopes. The adaptive immune system can recognize one or more epitopes of the same substance; as such, we differentiate between a monoclonal or polyclonal immune response (Abbas et al., 2018). Lymphocytes all differentiate from a common progenitor, and their activity can be crudely categorized as either direct or indirect; while T cells directly intervene in areas containing microbes or seemingly infected cells, representing the cell-mediated immunity, B cells produce antibodies and release them into the blood, constituting the humoral immunity. There is also a third, much smaller group of lymphocytes that cannot readily be categorized as either T or B cells, namely Natural Killer (NK) cells (Abbas et al., 2018). However, aside from their specificity and diversity, they all have certain features in common. During an adaptive immune response, all lymphocytes that come in contact with their antigen undergo clonal expansion – proliferating and massively increasing the number of cells expressing identical receptors for said antigen, i.e., they belong to one clone – to keep up with often rapidly dividing infectious pathogens (Abbas et al., 2018). Just as important as rapid activation, response, and expansion, is the adaptive immune system's ability to recede once a threat has been dealt with to avoid any further, unnecessary damage to the affected tissue. After an immune response, the immune system returns to a resting basal state called homeostasis (Abbas et al., 2018). This system is especially relevant for autoimmune diseases such as EAE and MS. These diseases are caused by the misidentification of molecules endogenous to the organism as foreign, pathogenic substances, effectively resulting in the body attacking itself, i.e., an auto-antigenic response, which leads us to the last important feature all members of the adaptive immune system share – tolerance. Several mechanisms exist in the body to maintain tolerance against self-antigens, including eliminating or inactivating lymphocytes that express receptors specific for self-antigens, or suppressing them with regulatory cells (Abbas et al., 2018). In EAE, these mechanisms do not apply, however, because the CNS is an immune-privileged site (Murphy & Weaver, 2017). Naïve lymphocytes, i.e., those who have yet to memorize an antigen, are never supposed to come in contact with molecules specific to the brain; however, this changes when animals are immunized with an exogenous protein like MOG by subcutaneous injection, thereby inducing EAE.

5.1 T lymphocytes

T lymphocytes, named so for their maturation in the thymus, are all positive for a certain glycoprotein on their cell surfaces, namely CD3, but can be divided into two main types depending on the expression of other such glycoproteins – $CD4^+$ helper T lymphocytes (Th cells) and $CD8^+$ cytotoxic T lymphocytes (CTLs). "CD" is the abbreviation for cluster of differentiation (Abbas et al., 2018; Schuhmacher, 2014).

5.1.1 Priming of T cells

A mature naïve T cell migrates through the cortical region of the lymph node until a pathogen-activated APC, typically a dendritic cell, binds to it. At least three types of signals are then deployed to activate the T cell. The first signal is the result of the interaction between a specific peptide:MHC complex and the T cell receptor (TCR), with subsequent stabilization of the structure through the co-receptors – either CD4 or CD8. However, this signal alone cannot drive proliferation and differentiation into an effector T cell on its own (Murphy & Weaver, 2017). Even if the first signal is received, the T cell will either be inactivated again or die altogether, after repeated stimulation without secondary signals (Abbas et al., 2018; Schuhmacher, 2014). As such, co-stimulatory signals promoting survival and expansion of the T cells and cytokines directing T cell differentiation into one of the different subsets of effector T cells are required (Murphy & Weaver, 2017). One such co-stimulatory signal is provided by B7 molecules, mainly CD80 and CD86, on the DCs' surfaces when they interact with the receptor CD28 on the naïve T cell, allowing for optimal clonal expansion, producing millions of T cells specific for one given antigen. This mechanism has a built-in negative feedback loop, as the activation of CD28 induces the synthesis of its own competitive inhibitor, CD152, featuring a 20-times more powerful affinity for B7 molecules. This loop is essential to prevent excessive activation (Murphy & Weaver, 2017). Finally, $CD4^+$ helper T cells – driven by cytokines synthesized by the activating APCs – differentiate into either Th1, Th2, Th17, or T regulatory (Treg) type cells (Abbas et al., 2018).

5.1.2 Effector T cells

Once differentiation is complete, T cells, except for those activating B cells, exit the lymphoid tissue into the blood to find target cells displaying their antigen. As they travel through the body, they bind to endothelial cells expressing adhesion molecules in response to inflammation and migrate into the infected tissue. When T cells encounter their antigen, they tightly bind to the infected cell and release their effector molecules (Murphy & Weaver, 2017).

5.1.3 $CD4^+$ helper T cells

Th1 cells

Th1 differentiation is primarily driven by the cytokines interleukin 12 (IL-12) and interferon gamma (IFN-γ), produced in response to various intracellular bacteria and some parasites that infect DCs and macrophages, as well as in response to viruses and antigenic proteins injected with strong adjuvants such as CFA. IL-12 is provided by macrophages and DCs and IFN-γ is initially provided by activated NK cells (Abbas et al., 2018). Differentiated

Th1 cells continue to synthesize IFN-γ which activates macrophages and DCs in their vicinity, enhancing Th1 cells' ability to kill intracellular microbes and present the antigen to further T lymphocytes. They can also secrete anti-microbial substances, such as TNF and lymphotoxin (Hohl, 2015).

Th2 cells

Th2 differentiation is primarily driven by interleukin 4 (IL-4) and is favored in response to helminths (parasitic worms) and allergens; by virtue of their persistent presence in the body, they cause chronic T cell stimulation, usually without a significant innate immune response. The absence of APCs and pro-inflammatory cytokines for vital differentiation into Th1 or Th17 cells causes the activated $CD4^+$ helper T cells to differentiate into Th2 cells (Abbas et al., 2018). Th2 cells are responsible for promoting B cell differentiation, antigen production, eosinophil recruitment, and mucus secretion (Hohl, 2015).

Th17 cells

Th17 were first discovered when researchers were looking for $CD4^+$ subpopulations that cause autoimmune inflammatory diseases in mice, such as EAE. Their involvement in EAE could be an indication that they also play a role in MS (Hohl, 2015). Th17 cells are capable of recruiting proinflammatory cells such as neutrophils and are important in the defense against extracellular cells and fungi. CFA containing M. tuberculosis used in the induction phase of EAE promotes Th17 production by virtue of two of the mycobacteria's cell wall components, namely trehalose dimycolate (aka. cord factor), a glycolipid, and peptidoglycan (aka. murein), a polymer of sugars and amino acids, which synergize to increase the Th17-promoting activity of mycobacteria (Hohl, 2015).

T regulatory cells (Treg)

Unlike Th1, Th2, and Th17 cells who are exclusively derived from naïve T cells during priming, T regulatory cells can either already emerge from the thymus as natural T regulatory cells (nTregs) or be induced during T cell priming as induced T regulatory cells (iTregs). Tregs are positive for CD25 as well as CD4 and, in mice, constitute 10% of all $CD4^+$ T cells; they ensure self-tolerance by suppressing the activation, proliferation, and effector functions of autoimmune T cells as well as the activation of macrophages and dendritic cells. (Hohl, 2015)

5.1.4 $CD8^+$ cytotoxic T cells (CTLs)

When a cell becomes infected with a virus or intracellular bacteria, the microbe itself is out of reach for the immune system. Even phagocytes with their internal microbicidal lysosomal machinery cannot destroy a microbe when it manages to enter the cytosol. As such, the only option left is to destroy the entire infected cell before the microbe can replicate within and spread to other, nearby cells. The cells of the adaptive immune system responsible for killing cells hosting microbes are the CTLs. Additionally, CTLs also play a vital role in the destruction of tumor tissue and are critically important for acute rejection of organ allografts (Abbas et al., 2018). The effector function of CTLs mainly entails the lysis of pathogen-infected

cells, and is triggered by MHC class I-dependent presentation of their corresponding antigen. The fastest mechanism antigen-activated CTLs can deploy is the targeted release of perforin granules together with granzymes, i.e., perforin/granzyme-mediated lysis; as the perforins destroy the plasma membrane, granzymes enter the cell and trigger apoptosis. Alternatively, CTLs can trigger apoptosis by expressing the Fas ligand, which binds to Fas on the target cell's surface, i.e., Fas-mediated death. CTLs have also been shown to secrete IFN-γ and TNF, allowing them to recruit macrophages and neutrophils (Hohl, 2015). Naïve $CD8^+$ T cells do not contain the machinery to destroy other cells or synthesize IFN-γ and TNF until they are activated. While $CD8^+$ T cell activation happens mostly analogous to $CD4^+$ T cell activation, it seems to additionally require aid from specialized dendritic cells and, in case of a weak initial immune response, $CD4^+$ T cells that area already activated. This is because most viruses cannot infect DCs but DCs are the most reliable activators of T cells. To facilitate the response, the immune system utilizes a mechanism called cross-presentation: specialized DCs ingest infected cells, tumor cells, or proteins synthesized by these cells, transfer the antigens into the cytosol, and process them for MHC I-mediated presentation (Hohl, 2015). CTLs seem to be the main driving force behind the destruction of myelin, at least in the early stages of MS (Mars et al., 2011).

5.2 B lymphocytes

While T cells mature in the thymus, naïve B cells mature in the bone marrow. They express membrane-bound immunoglobulins (mIgs) – so-called B cell receptors (BCRs) – on their surfaces to recognize their antigen (Murphy & Weaver, 2017). These mIgs are represented by mIgM and mIgD on naïve B cells and mIgG on memory B cells (Li et al., 2019). BCRs can recognize both non-protein and protein antigens, the latter notably in their native form. B cell activation with antigens of protein origin requires the aid of T cells (Abbas et al., 2018).

5.3 Natural killer (NK) cells

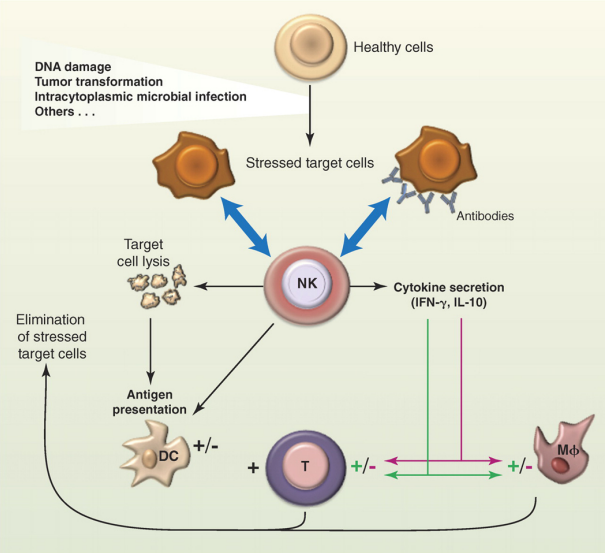

Figure 5.1: NK cells recognize a variety of stress signals from cells in both absence and presence of antibodies. Once activated, NK cells can then lyse target cells and produce various cytokines and chemokines depending on the nature of the stimulation. NK cells might also interact with DCs in various ways, such as killing immature ones or promoting their maturation, leading to enhanced antigen presentation for T cells. In this figure, NK cells stimulate or inhibit macrophage and T cell activity through IFN-γ or IL-10 secretion, respectively. Republished with permission of American Association for the Advancement of Science, from Vivier, E., Raulet, D. H., Moretta, A., Caligiuri, M. A., Zitvogel, L., Lanier, L. L., Yokoyama, W. M., & Ugolini, S. (2011). Innate or adaptive immunity? the example of natural killer cells. *Science (New York, N.Y.)*, 331(6013), 44–49; permission conveyed through Copyright Clearance Center, Inc.

NK cells constitute the third type of lymphocytes; however, despite many characteristics they have in common with T and B lymphocytes, they are generally not considered part of the adaptive immune system. Due to new evidence in recent years, they are not fully considered part of the innate immune system, either (Vivier et al., 2011). Originally, NK cells were defined as the effector lymphocytes of the innate immune system with cytolytic capabilities in the absence of specific immunization. However, they have been shown to express a range of activating and inhibiting receptors that both ensure self-tolerance and increase effectiveness in defending against virus infection and tumors (Vivier et al., 2011). They are major producers of TFN-γ and can also synthesize other cytokines, both pro-inflammatory and immunosuppressive, such as TNF-α and IL-10, respectively. Like macrophages, DCs, and other APCs, NK cells are also capable of secreting various chemokines allowing them to direct other immune cells to sites of infection or inflammation (Abbas et al., 2018; Vivier et al., 2011). By virtue of the combination of NK cells' cytolytic function as well as their ability to secrete cytokines, they impact DCs, macrophages, and neutrophils, and have influence over subsequent T and B cell responses; as such, NK cells appear to represent a regulator for both innate and adaptive immune system (Vivier et al., 2011). As NK cells patrol around the body, they contact other cells at a high frequency and, depending on the ratio of activating

and inhibiting signals, destroy or continue. NK cells have activating receptors recognizing molecules associated with tumor growth or antibody-mediated stress and inhibiting receptors recognizing cognate MHC I, ensuring self-tolerance; tumorous and infected cells often lose the ability to express MHC I, making them a target for NK cells. When the NK cell is activated it unidirectionally releases cytotoxic granules containing perforin and granzymes analogously to CTLs (Eissmann, 2021). Contrary to what was previously assumed, NK cells have been demonstrated to exhibit some type of memory in viral infections. Considering the studies by Dokun in 2001 and Cooper in 2008, mature NK cells may acquire stable, heritable features that influence their activity upon reinfection (Cooper et al., 2009; Dokun et al., 2001; Vivier et al., 2011).

5.3.1 Natural killer T (NKT) cells

NKT cells represent a small subset of T cells that express a limited range of TCRs compared to other T lymphocytes in combination with typical NK cell markers. They can recognize glycolipid antigens presented by the non-typical MHC protein CD1d. Their capabilities in terms of cytotoxicity and cell signaling are analogous to NK cells (Hohl, 2015; Kumar et al., 2017).

5.4 Antibodies

Antibodies, i.e., immunoglobulins (Ig), are proteins that circulate through the blood and bind to specific epitopes on supposed microbes. They are considered mediators of humoral immunity against all types of pathogens, and exist in two forms: membrane-bound on a B cell's surface where they act as antigen-specific receptors, or secreted into the blood serum to recognize and bind to their antigen upon contact (Abbas et al., 2018).

All antibodies are Y-shaped and have much of their basic structure in common; however, they exhibit vast variability in the antigen-binding regions. Their effector functions and physiochemical features depend on the non-antigen-binding portion, i.e., the constant (C) domain, which is much more limited in its variance. There are 5 isoforms of immunoglobulins that are distinguished by their C regions: IgM, IgD, IgG, IgA, and IgE (Abbas et al., 2018; Janeway, 2001). The symmetric core structure of antibodies consists of two identical heavy and two identical light chains forming three equally sized portions loosely connected by a flexible tether (Abbas et al., 2018; Janeway, 2001). The Fragment crystallizable (Fc) region represents the stem of the antibody, determines its isoform, and is fully formed by parts of the heavy chains. The Fc region is also the point of attachment for Fc receptors (FcRs) on immune cells – resulting in recruitment of said cells. Two identical antigen-binding fragments (Fab) regions form the arms of the antibody and end in the so-called variable regions that give it its specificity for an antigen epitope. The Fab regions are made part heavy chain and part light chain and can move independently from each other thanks to the flexible hinge region that connects the Fab and Fc regions (Janeway, 2001). IgGs represent the vast majority of antibodies in the body at about 75% and exhibit the longest half-life of all antibodies. They do not form polymers and can be divided into four subclasses – IgG_1, IgG_2, IgG_3, and IgG_4 ranked by abundance in the blood. IgGs are capable of recruiting the complement system, resulting in opsonization as well as immune cells. However, IgGs can also incapacitate or neutralize a microbe or toxin by themselves when they attach to it in large numbers, especially if they

bind to a different microbial particle with either antigen-binding region, cross-linking them (Dutta, 2018; Schroeder & Cavacini, 2010).

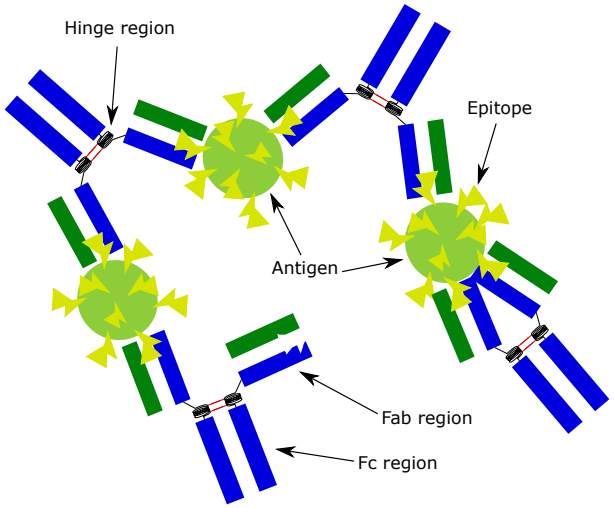

Figure 5.2: Antibody-antigen cross-linking. The hinge region of an antibody molecule opens and closes allowing better binding between the antibody and antigen epitope. This also facilitates cross-linking of antigens into larger antigen-antibody complexes.

Antibody glycosylation modifies the Fc region and determines which Fc receptors it can bind to for recruitment of effector cells (Jennewein & Alter, 2017). This post-translational modification leads to the addition of N-glycans at specific asparagine residues on an antibody's heavy chain causing changes in conformation and enhancing stability. As such, antibody glycosylation represents the final step of fine-tuning of an immunoglobulin's biological activity (Irvine & Alter, 2020). There is a large array of different FcRs and complement proteins – summarized as antibody sensors – essential to combat infection and regulate immunity. These sensors interact with different subtypes of antibodies depending on the molecular features of their Fc regions (Irvine & Alter, 2020).

Fc-glycosylation is determined by certain T cell-associated cytokines, as they regulate glycosyltransferase expression in B cells (Pfeifle et al., 2017). The four types of glycosylation modification are fucosylation, bisection, galactosylation, and sialylation (Irvine & Alter, 2020). All types of glycosylation take place at the so-called core glycan, which comprises two consecutive N-acetylglucosamine (GlcNAc) residues followed by a mannose residue which is in turn followed by two mannose antennae ending in a single GlcNAc residue each. This core glycan is then sequentially modified further by a set of four glycosyltransferases (Irvine & Alter, 2020).

Fucosylation is the most common type of glycosylation. Over 90% of IgG in serum of healthy individuals has a core fucosylation in their Fc region. Complete loss of fucosylation increases IgG-Fc affinity for FcγRIIIα (CD16a) fifty-fold. FcγRIIIα is highly expressed on NK cells which engage in excessive antibody-dependent cellular cytotoxicity (ADCC) and inflammatory activity upon activation by afucosylated IgGs (Gudelj et al., 2018; Irvine & Alter, 2020). Bisection is caused by glycosylation with GlcNAc and appears in about 10% of circulating IgG. The addition of GlcNAc to the core glycan can inhibit both fucosylation and galactosylation. Additionally, it increases affinity for FcγRIIIα as well, though not as

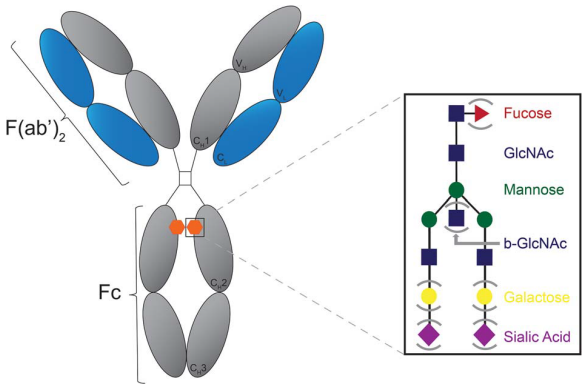

Figure 5.3: Structure of IgG and the IgG N-linked glycan. IgG molecules have a single N-linked glycosylation site at asparagine 297 (in humans) or asparagine 174 (in mice) of each heavy chain. The base glycan structure is depicted, with each of the four variably added glycan moieties present in parentheses. Republished with permission of Oxford University Press - Journals, from Irvine, E. B. & Alter, G. (2020). Understanding the role of antibody glycosylation through the lens of severe viral and bacterial diseases. *Glycobiology*, 30(4), 241–253; permission conveyed through Copyright Clearance Center, Inc.

highly (Gudelj et al., 2018). Galactosylation is also a relevant modification when it comes to multiple sclerosis and similar diseases. While agalactosylation, monogalactosylation, and digalactosylation account for about 35%, 35%, and 15% of circulating IgG, respectively, this ratio is significantly shifted to agalactosylation in patients with autoimmune and inflammatory diseases. Agalactosylation is associated with proinflammatory signaling, but it is not known to what extent it should be considered cause or consequence (Irvine & Alter, 2020). On the other hand, studies have shown that Fc-galactosylation of IgGs enhances classical complement activation and complement-dependent cytotoxicity (Peschke et al., 2017; van Osch et al., 2021).

Chapter 6

Etiology, clinical course, & pathology of MS & EAE

6.1 Etiology

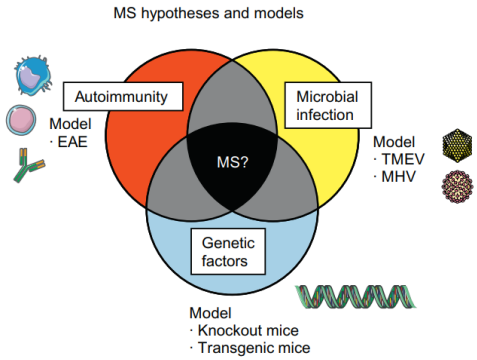

Figure 6.1: The etiology of MS has several hypotheses. The most common hypotheses involve microbial infections, autoimmune responses, and genetic factors. Theiler's murine encephalomyelitis virus (TMEV) and murine hepatitis virus (MHV) infections are used as viral models of MS, while EAE is an autoimmune model for MS. Republished with permission of Elsevier, from Sato, F., Omura, S., Martinez, N. E., & Tsunoda, I. (2018). Chapter 3 - animal models of multiple sclerosis. In A. Minagar (Ed.), *Neuroinflammation (Second Edition)* (pp. 37–72). Academic Press, second edition edition; permission conveyed through Copyright Clearance Center, Inc.

MS and EAE are both inflammatory demyelinating diseases of the CNS. As of today, we do not know the exact cause of MS; however, it has been proposed to be the result of autoimmunity, microbial infections, and/or genetic factors (Sato et al., 2018). EAE only accounts for one of these three hypotheses: autoimmunity. Clinically, there have been various findings that support the autoimmune etiology of MS, such as anti-myelin T cells and antibodies found in certain patients, T cell and macrophage infiltration of and antibody deposition at demyelinating lesions as well as the efficacy of immunosuppressive drugs such as natalizumab (Lassmann et al., 2001; Sato et al., 2018). Viral infections have also been implicated in MS pathogenesis in studies demonstrating the presence of viruses and antiviral immune responses

in MS patients. Experimentally, researchers have successfully induced demyelinating diseases by viral infection (Baumgärtner & Alldinger, 2005; Opsahl, 2005; Sato et al., 2018). The single most influential genetic factor in the development of MS is sex. The ratio between women and men is 2.3-3.5:1. Other genetic factors such as genes for certain interleukins and receptors thereof have also been implicated to affect the likelihood of developing MS (Sato et al., 2018). It should be noted that sex and the genetic element to MS is still relevant to EAE, as different mouse strains have exhibited some major differences in pathology and progression of as well as recovery from EAE (Sato et al., 2018).

6.2 Clinical course

The clinical course of MS is classified into four types: relapsing-remitting (RR), primary progressive (PP), secondary progressive (SP), and clinically isolated syndrome (CIS). CIS is a relatively new classification and one of the original classes, progressive-relapsing MS, is now considered a type of primary progressive MS (Sato et al., 2018). CIS is defined as a potentially isolated incident of neurological symptoms often associated with MS – the operative word being "potentially" – as it might be the first sign of the patient developing MS (Efendi, 2016). RR-MS entails the alternation between bouts of neurological symptoms and recovery, this type of MS represents 85%-95% of all cases of MS. In SP-MS, patients show a typical RR-MS course with subsequent progression of the disease; 95% of RR patients eventually turn out to develop SP-MS. In PP-MS, the disease progresses continuously without any periods of recovery. PR patients experience continuous progression with bouts of acute relapses in between. Studies on RR-MS patients have shown an association with balance between Th cell subtypes. In mice, MBP-EAE has shown a similar progression to human CIS, while PLP-EAE is a model for RR-MS. Some types of MOG-EAE have the special feature of showing not only T cell but also antibody (i.e., B cell) involvement. Studies have shown that B cells cannot induce EAE on their own, but they seem to contribute to its pathogenesis by facilitating T cell reactivation in the CNS (Pierson et al., 2014; Sato et al., 2018). C57BL/6 mice are the preferred strain for models investigating a chronic-progressive course (i.e., PP and SP) (Chastain et al., 2011; Sato et al., 2018).

6.3 Pathology – $CD4^+$ T cells in MS & EAE

Even though $CD8^+$ T cells constitute about 80% of T cells in early active lesions in MS, Th cells still seem to play a central role as well.

MS has previously been proposed to be Th1-mediated, since Th1 cells produce large quantities of inflammatory cytokines and their activity correlates with the pathogenesis of EAE. Additionally, adoptive transfer of autoantigenic Th1 cells can sufficiently induce passive EAE (Merrill et al., 1989; Sato et al., 2018).

Th2 differentiation includes a mechanism that inhibits Th1 differentiation and function(Abbas et al., 2018). Adoptive transfer of PLP-specific Th2 cells into PLP-sensitized mice prevents them from developing EAE (Constantinescu et al., 2001; Kuchroo et al., 1995; Sato et al., 2018). Mice overexpressing GATA-3, an essential transcription factor for Th2 differentiation, have also been shown to experience less severe symptoms in MOG-induced EAE compared to wild-type mice (Fernando et al., 2014). However, in MOG-EAE involving

antibody deposition, Th2 cell activity has also shown to promote autoantibody production resulting in a type of secondary progressive EAE (SP-EAE) (Tsunoda et al., 2005).

Th17 cell count is increased in peripheral blood, brain lesions, and cerebrospinal fluid (CSF) of MS patients (Matusevicius et al., 1999; Sato et al., 2018). Th17-deficient mice have also been shown to have delayed onset and decreased severity of EAE after immunization with MOG compared to wild-type (Komiyama, 2006, Sato, 2018). A study by O'Connor et al. from 2008 showed that Th17 cells cannot cause EAE by themselves, but require lesions produced by Th1 cells first to enter the brain (O'Connor et al., 2008); however, this finding is in direct conflict with a study by Jäger et al. from 2009 claiming that adoptive transfer of MOG-specific Th17 cells causes EAE of comparable severity to MOG-specific Th1 cells, though with different, yet overlapping pathologies (Jäger et al., 2009). Tregs make up between 4% to 10% of $CD4^+$ T cells in mice compared to 2% to 5% in humans. They can suppress proliferation of and cytokine production by effector T cells (Sato et al., 2018). Adoptive transfer of Tregs harvested from naïve mice together with MOG-specific T cells has an alleviating effect on MOG-EAE when compared to exclusive transfer of MOG-specific T cells (Kohm et al., 2002).

In conclusion, there is ample evidence on which Th subsets can play a detrimental and protective role in MS and EAE; however, the answer as to which among these subsets contribute to the development of such autoimmune diseases, especially to the development of MS, still eludes us. Generally, animal models have shown that Th1 and Th17 produce induction and relapse, while Th2 and Tregs are important for prevention and remission. However, effector mechanisms such as Th2 cells' ability to promote autoantibody production have also been demonstrated to contribute to certain MS subtypes and progressive EAE models (Tsunoda et al., 2005; Sato et al., 2018).

6.4 Differences between MS & EAE

There is no single type of EAE that can stand as a holistic model for MS. There are multiple reasons for this: the multifactorial nature and heterogenicity of MS is the most obvious; however, we also need to consider the animals used. Aside from the human immune system being generally much more robust compared to those of rodents, there are several other differences, such as in the ratio of different cell types, disparities in capabilities and functions within the same cell types as well as different effects of analogous signaling molecules and balance between innate and adaptive immune response. For instance, while the human blood is much richer in neutrophils, the perivascular cuffs that form in the CNS of EAE mice show a significantly higher ratio of neutrophils when compared to cuffs in MS patients where mononuclear cells are the predominant cell type (Mestas & Hughes, 2004). Also, MS occurs spontaneously while EAE is artificially induced and the time frames on which the diseases develop are vastly different. In mice, EAE develops days after inductions with first symptoms appearing after less than two weeks, while MS takes years. There is still no definitive explanation as to why the time frames differ so dramatically (Friese et al., 2006; Schuhmacher, 2014). However, all differences aside, EAE is still the most commonly used and most likely the most viable model for MS we have today.

Chapter 7

MOG antibody-associated disease (MOGAD)

While MOG-EAE has primarily been used as an MS model it has more recently also been used as a model for a much more closely related disease in humans: MOGAD (Ambrosius et al., 2020). Unlike in most autoimmune diseases, MS included, MOGAD has a gender ratio close to 1:1 and is more common in children than adults (Hor et al., 2020). MOGAD is commonly associated with recurrent optic neuritis, transverse myelitis, and/or acute disseminating encephalomyelitis (Ambrosius et al., 2020; Chen et al., 2018; Wynford-Thomas et al., 2019). There is still some overlap with MS, as optic neuritis has been associated with both diseases (Ambrosius et al., 2020; Chen et al., 2018; Kale, 2016). Interestingly, while symptomatically, MOGAD is more closely related to another disease, namely neuromyelitis optica spectrum disorder (NMSOD), where autoantibodies destroy aquaporin 4 proteins (Ambrosius et al., 2020; Chen et al., 2018), the underlying immunopathology is more closely related to MS (Ambrosius et al., 2020; Zheng et al., 2021). Lennart Mars investigated the effects of antibody afucosylation on EAE course, which is more typical for MOGAD than MS. Similar experiments could be set up to investigate MS, as it has been more closely associated with different aberrant Fc-glycosylation patterns, namely increased bisection by GlcNAc and agalactosylation (Mars, 2020). However, both fucosylation as well as bisection and agalactosylation increase affinity for FcγRIIIα (Irvine & Alter, 2020), making this project relevant to both MOGAD as well as MS.

Chapter 8

Aim

The principal aim of this thesis is to determine how fucosylated and afucosylated IgG glycovariants affect immune activity and pathology in the spinal cords of C57BI/6 mice with actively induced MOG_{35-55}-EAE. It covers whether there are any changes in terms of extent of demyelination, inflammation, and/or changes in the phenotypes of infiltrating cells, such as the presence of NK, NKT, T, and B cells. The desired outcome is insight into the processes involved in autoimmune diseases such as MOGAD and MS.

Part II

Methods

Chapter 9

Animal selection, treatment & sacrifice

Animal selection, treatment and sacrifice, and clinical scoring were performed at the laboratory of Dr. Lennart Mars at the Lille Neuroscience & Cognition Institute. Stains and quantitative evaluation were performed at the Department of Neuroimmunology at the Center for Brain Research in Vienna.

Mouse anti-MOG recombinant antibody - Clone 8-18C5

Clonal antibodies that only differ in their glycosylation profile were used. Lennart Mars and his team utilized the mouse monoclonal antibody (mAb) 8-18C5 IgG_1, which causes immune-mediated demyelination. It first induces direct complement-mediated demyelination by binding to MOG. Additionally, its formation of immune complexes with MOG marks it for FcR-mediated phagocytosis with subsequent antigen recall-associated T-cell pathogenicity. Another important feature of 8-18C5 is that it binds to a conformational epitope on MOG, i.e., it exclusively interacts with native MOG, not the MOG-derived peptide $MOG_{35\text{-}55}$ used to induce active EAE (Breithaupt et al., 2003; Flach et al., 2016; Mars, 2020). The constructed recombinant 8-18C5 mAb was produced in different mammalian cell lines imposing different glycosylation profiles: human embryonic kidney 293 cells (HEK) and Chinese hamster ovary cells (CHO) which exhibit high rates of fucosylation as well YB2/0 cells which are $FUT8^{-/-}$, i.e., fucosyltransferase 8-deficient, and hence perform little fucosylation. Fc-glycosylation on IgG_1 in mice is associated with the asparagine residue 174 (N174). HEK cells produced a traditional biantennary core glycan (G0F) in 77% of N174, while CHO produced three predominant glycoforms, namely G0F, G1F, and non-glycosylated N174 at a rate of 42%, 21%, and 27%, respectively. YB2/0 cells predominantly produced a traditional biantennary core glycan in 80% of IgG which in turn exhibited glycovariant G0F in 50% and G0, i.e., the non-fucosylated variant, in 45% of cases, respectively. In other words, YB2/0 cells produced fucosylated (G0F) IgG_1 at only half the rate of HEK cells. To ensure the antibodies were otherwise identical, the same expression vector was used for all of them, making them equally affine for MOG (Mars, 2020).

Chapter 10

Clinical scoring, evolution, & recovery

Clinical scoring was determined according to the following table.

Table 10.1: Clinical scoring

Score	Description
0	No clinical signs
1	Tail weakness or simple delay in turning over
2	Absence of straightening with tail weakness
3	Paralysis of one of the two lower limbs
4	Severe paralysis of the lower limbs
5	Quadriplegia
6	Moribund state or death

Clinical evolution, survival, recovery, and cumulative disease score were determined. The clinical evolution is used to determine the clinical score over time, recovery is defined as the persistent absence of neurological symptoms (EAE score 0), and cumulative disease score represents the sum of all daily disease scores for each mouse.

Chapter 11

Sample preparation

11.1 Sample extraction & paraffin infiltration

Cerebral cortex, cerebellum, spinal cord, nervus opticus, and a section of the spleen (the last as a positive control for lymphocyte stains) were isolated. The cerebral cortex was sectioned into three coronal segments; the cerebellum was sectioned analogous to the cortex into two segments. The spinal cord was sectioned into several transverse segments with a length of 3 to 5 mm each. The samples were subsequently embedded in paraffin, and cross-sections of 2-5 micrometers were shaved off using a slide microtome and prepared on object slides for staining.

11.2 Deparaffinization

All following steps were performed at room temperature. Formalin-fixed paraffin-embedded (FFPE) sections of the samples mounted on microscope slides were incubated in xylene for 15 min twice, to remove the paraffin and subsequently briefly washed in 96% Ethanol. If necessary for the following stain, endogenous peroxidase activity was blocked by submersion in Methanol/H_2O_2 for 30 min. Afterwards, the samples were rehydrated in an alcohol series of descending concentrations (96%, 70%, 50%) and finally distilled water.

Chapter 12

Histological stains

12.1 Hematoxylin-eosin (HE)

Rehydrated samples were incubated in Mayer's hemalaun for 5 min for nuclear staining. After washing the samples with tap water, samples were differentiated in HCl-ethanol before being washed again. Sections were then put in Scott's solution for 5 min and once again washed. Incubation in eosin for 4 minutes led to cytoplasmic staining and was once again followed by washing. Samples were dehydrated through an ascending ethanol series (50%, 70%, 2x96%) and n-butyl acetate. Finally, coverslips were put on the slides using Eukitt as mounting medium.

12.2 Luxol fast blue-periodic acid schiff (LFB-PAS)

Rehydrated samples were incubated in 0.1% Luxol Fast blue at 57°C overnight. After cooldown, the samples were rinsed with 96% ethanol and distilled water. For the PAS-reaction, the samples were exposed to 0.8% periodic acid for 10 min, washed with distilled water, then submerged in Schiff's reagent for 30 min, followed by 3 sulfite washing solutions, 2 min each. After rinsing with tap water, the process was analogous to HE staining with dehydration, n-butyl acetate, and mounting with Eukitt.

12.3 Immunohistochemical stains (IHC) & fluorescent stains

12.3.1 Chromogenic immunohistochemistry (CIH)

All immunolabeling was done using a secondary antibody system and, where appropriate, a biotin-avidin system.

After deparaffinization, heat-induced epitope retrieval (HIER) was performed by steaming the samples submerged in either EDTA pH 8.5 or citrate buffer pH 6.0 (depending on the epitope) for 60 min. The samples were left to cool for about 15 min before being rinsed with TBS. Unspecific background reactions were preemptively prevented by 15 min treatment with 10% Fetal calf serum (FCS) in DAKO buffer. Primary antibodies were diluted in 10% FCS/DAKO buffer according to Table 12.1 and applied at 4°C overnight. After rinsing once again, the secondary antibodies – diluted in 10% FCS/DAKO buffer according to Table 12.2

– were applied for 1 h at room temperature. After another TBS rinse, avidin-horseradish peroxidase (HRP) in 10% FCS/ DAKO-buffer at dilution 1:500 was applied for 1 h at room temperature as well. Finally, the samples were rinsed with TBS again and developed with 3,3'-Diaminobenzidine (DAB) or 3-amino-9-ethylcarbazole (AEC). Alternatively, avidin-alkaline phosphatase (AP) was used to develop with Fast Blue or Fast Red, instead. For DAB, Eukitt was used as mounting medium, for dyes such as AEC, Fast Blue, and Fast Red, Geltol was used. CIH was performed for either single or double labeling. In case of double labeling, the two markers were stained in sequence, with 30 min steaming in between to remove the first set of antibodies before applying the next.

The three antibody combinations in double stains were CD3(SP7)+CD8a for differentiation between $CD4^+$ and $CD8^+$ T cells, EOMES+Granzyme B (GrB) for NK cells (which was not reliable), and CD3(SP7)+CD161c for differentiation between NK and NKT cells.

12.3.2 Catalytic signal amplification (CSA)

When necessary, amplification with biotinylated tyramide was performed by introducing two intermediate steps. Immunostaining was performed analogous to the standard protocol until the addition of avidin-peroxidase. After this step, biotinylated tyramide and H_2O_2 (30%) were diluted in PBS at a ratio of 1:1:1000 and applied to the samples for 20 min at room temperature. After a PBS wash, the appropriate avidin-substrate/dye conjugate was applied for 30 min at room temperature. The samples were then rinsed with TBS before finally being developed and/or covered.

12.3.3 Immunofluorescence

Immunofluorescent stains were exclusively performed for demonstrative purposes. Unlike CIH, immunofluorescent labeling does not involve catalytic reactions; the fluorophores are directly conjugated with the secondary antibody or avidin; aside from that, all other steps were identical, though light sensitivity had to be accounted for. Primary and secondary antibodies were diluted in 10% FCS/ DAKO buffer according to Tables 12.3 and 12.4, respectively. When no CSA was required and primary antibodies were from different species they were applied simultaneously, while secondary antibodies were always applied together.

Three immunofluorescent triple stains were produced to differentiate between T, NK, and NKT cells:

- CD3(SP7)+GrB+CD8
- CD3(CD3-12)+GrB+EOMES
- CD3(CD3-12)+CD161c+GrB

Another triple stain – PLP+CD8a+GrB – was produced to visualize CTLs/regulatory T cells and NK cells in lesions of demyelinated white matter.

Antibodies used in CIH stains

Table 12.1: Primary antibodies used in CIH stains

Antibody	Dilution	Pretreatment	CSA	Type	Target	Manufacturer
CD3 (Clone SP7)	1:1000	EDTA pH 8.5	Yes	Rabbit, monoclonal	T cells	Thermo Fisher Scientific
CD8a	1:1000	EDTA pH 8.5	No	Rabbit, monoclonal	NK cells, CTLs, Tregs	Abcam
Granzyme B	1:250	EDTA pH 8.5	No	Goat, polyclonal	NK cells, CTLs	R&D Systems
EOMES/Tbr2	1:500 (DAB) 1:250 (FB)	EDTA pH 8.5	No	Rabbit, polyclonal	NK cells, radial glia, developing neurons	Abcam
CD161c/Klrb1c (E6YG9)	1:200	EDTA pH 8.5	No	Rabbit, polyclonal	NK cells, NKT cells	Cell Signaling Technology
CD45R/B220	1:250	Citrate	No	Rat, monoclonal	B cells	BD/ Pharmingen

Table 12.2: Secondary antibodies used in CIH stains

Antibody	Dilution	Type	Target	Manufacturer
Biotin-anti-rabbit	1:1000	Donkey	Rabbit IgG	Jackson ImmunoResearch
Biotin-anti-goat	1:250	Donkey	Goat IgG	Jackson ImmunoResearch
Anti-rabbit-AP	1:100	Donkey	Rabbit IgG	Jackson ImmunoResearch
Anti-rabbit-HRP	1:1000	Donkey	Rabbit IgG	Jackson ImmunoResearch
Avidin-AP [1]	1:500	Avidin	Biotin	Jackson ImmunoResearch

[1] Avidin-alkaline phosphatase is technically not an antibody

Antibodies used in immunofluorescent stains

Table 12.3: Primary antibodies used in immunofluorescent stains

Antibody	Dilution	Pretreatment	CSA	Type	Target	Manufacturer
CD3 (Clone SP7)	1:1000	EDTA pH 8.5	Yes	Rabbit, monoclonal	T cells	Thermo Fisher Scientific
CD3 (CD3-12)	1:100	EDTA pH 8.5	Yes	Rat, polyclonal	T cells	AbD Serotec
Granzyme B	1:50	EDTA pH 8.5	No	Goat, polyclonal	NK cells, CTLs	R&D Systems
CD8a	1:250	EDTA pH 8.5	No	Rabbit, monoclonal	NK cells, CTLs, Tregs	Abcam
EOMES/Tbr2	1:100	EDTA pH 8.5	No	Rabbit, polyclonal	NK cells, radial glia, developing neurons	Abcam
PLP	1:2500	EDTA pH 8.5	Yes	Rabbit, polyclonal	Myelin	Abcam

Table 12.4: Secondary antibodies used in immunofluorescent stains

Secondary Antibody	Dilution	Type	Target	Manufacturer
Biotin-anti-rabbit	1:1000	Donkey	Rabbit	Jackson ImmunoResearch
Cy2-avidin[2]	1:100	Avidin	Biotin	Jackson ImmunoResearch
Cy2-anti-goat	1:100	Donkey	Goat	Jackson ImmunoResearch
Cy3-anti-goat	1:100	Donkey	Goat	Jackson ImmunoResearch
Cy3-anti-rabbit	1:200	Donkey	Rabbit	Jackson ImmunoResearch
Cy5-anti-rabbit	1:200	Donkey	Rabbit	Jackson ImmunoResearch
Cy5-anti-rat	1:100	Donkey	Rat	Jackson ImmunoResearch

[2]Cy2-avidin is technically not an antibody

Chapter 13

Quantitative evaluation

13.1 Demyelination

Demyelination was measured with light microscopy using a Luxol stain and evaluated as a percentage of total white matter using a ten-by-ten morphometric grid. Six to ten cross-sections per animal were used and the mean percentage of demyelination between them calculated. Myelin is essential for efficient signal transduction, especially in the motor system; as such, demyelination might be one of the clearest association between clinical score and neuropathological changes.

13.2 Inflammatory index

Using an HE stain, this parameter is measured as the average number of blood vessels with perivascular location of inflammatory cells, i.e., perivascular cuffs, per spinal cord cross section. The number of perivascular cuffs was evaluated in six to ten cross sections per animal and the number of cuffs per cross section determined by calculating the mean. The inflammatory index is a good indicator for immune activity and potentially impending demyelination that would have taken place had the animal not been sacrificed.

13.3 Manual counting of cells

13.3.1 NK & NKT cells

A double stain for CD161c and CD3 to stain for NK ($CD161c^{+}CD3^{-}$) and NKT ($CD161c^{+}CD3^{+}$) cells was performed and their numbers within the perivascular space and parenchyma of the spinal cord were counted. Six cross sections were evaluated per animal, with both surface area of the sections (using the morphometric grid) as well as $CD161c^{+}CD3^{-}$ and $CD161c^{+}CD3^{+}$ cell numbers (using a differential tally counter) being measured; subsequently, the number of all $CD161c^{+}$ cells per mm2 and the prevalence of the NKT cells among $CD161c^{+}$ cells as a percentage were calculated. NK and NKT cells are capable of detecting antibodies bound to microbes and cells, allowing them to engage in ADCC.

13.3.2 B cells

B cells in the perivascular spaces and parenchyma of the spinal cord were labeled with an antibody against B220, an isoform of CD45. Analogous to NK and NKT cells, six cross sections per animal were evaluated with surface area and cell count in the perivascular space and parenchyma of the spinal cord being measured, and subsequent calculation of B cell count per mm2. While this antigen is only present on a certain subset of B cells but also on some T cells in humans, it is a specific pan-B cell marker in mice. B cells' ability to produce antibodies and attract other immune cells could contribute to clinical symptoms and neuropathology.

13.3.3 Ratio between different T cell populations

A double stain for CD3 and CD8 was performed to evaluate the prevalence of $CD4^+$ T cells among all T cells within the spinal cord parenchyma and perivascular space. CD3 is the antigen used to label all T cells, i.e., Th cells, Tregs, CTLs, and NKT cells. CD8a is one of the two subunits comprising the heterodimer CD8αβ or the homodimer CD8αα; aside from CTLs, NK cells and regulatory T cells stain positive for CD8a as well. $CD3^+CD8^-$ and $CD3^+CD8^+$ cells were counted using a differential tally counter until 300 total cells were tallied for each animal and prevalence of $CD4^+$ helper T cells ($CD3^+CD8^-$) among all T cells ($CD3^+CD8^{+/-}$) was evaluated as a percentage.

13.3.4 Counting of T cells by imaging software analysis

T cells penetrated into the CNS in such great numbers that a manual count of their absolute number would have invited errors. Hence, T cell stains for CD3 were scanned and digitized for software analysis. Six cross sections were evaluated per animal. First, the surface area of each cross section was determined using the annotation function of the software NDP.view. The image was then exported for T cell count throughout the entire spinal cord parenchyma and perivascular space using Image-Pro Premier. In Image-Pro Premier, the smart segmentation tool was used. This allowed for the definition of what should be considered positive signal and what should be considered background. This involved initially selecting 3 to 5 representative T cells manually as regions of interest in each of the cross sections and then selecting examples for background signal, i.e., regions and cells negative for CD3, namely, connective tissue, blood vessels, artifacts, and $CD3^-$ cells. When the first example of background signal was selected, the software automatically produced a preliminary overlay illustrating which areas it would consider T cells and which it would consider background. The more examples are selected, the more accurate the detection becomes. Once a sufficient number of examples had been selected (about 6 to 10 T cells and 2 to 3 background signals per cross section), detection was refined further by excluding signals smaller than 5 μm^2. Before counting, the regions to be counted had to be selected; each of the cross-sections was defined and the button "Count" selected. Lastly, once the count was finished, the "Split" function was utilized using the option of automatic watershed-based splitting which allows the program to separate large accumulations of T cells into individual cells. The final count of cells was then divided by the total surface area of all six cross sections to determine T cells/mm^2, which was used for statistical evaluation.

13.4 Confocal microscopy

Immunofluorescent stains were scanned using the Leica SP5 II Laser Scanning Confocal Microscope. The images produced this way were then processed using ImageJ and Photoshop to make different markers clearly discernable.

13.5 Statistics

Aided by the program GraphPad Prism 9, ordinary one-way ANOVA was used for statistical analysis and illustration, correcting for the multiple comparisons between each of the groups and controls with Dunnett's correction.

Part III

Results

Chapter 14

Clinical score, survival & recovery

In this thesis we analyzed the spinal cord with a series of experiments in which C57BI/6 mice with MOG_{35-55}-induced EAE were treated with additional intravenous transfer of glycovariants of an IgG_1 antibody against MOG.

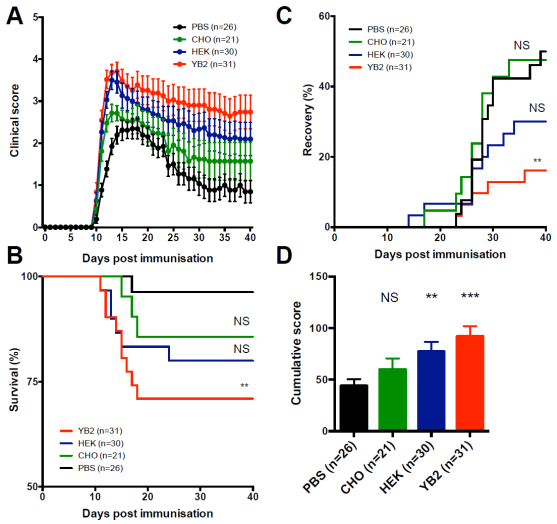

Figure 14.1: YB2/0 increased maximal clinical score (A) and cumulative score (D) with reduced survival (B) and recovery rate (C).

Treatment of these animals with different glycovariants by Lennart Mars and his team in Lille led to significant differences in clinical disease. Treatment with glycovariants originating from CHO, HEK, and YB2/0 cells increased maximal clinical scores. Additionally, clinical scores decreased much slower over time compared to controls only treated with PBS (Figure 14.1A). Treatment with YB2/0 glycovariants also had a detrimental effect on survival rate, reducing it by more than 25% (Figure 14.1B); similarly, recovery was significantly limited in mice treated with YB2/0 glycovariants (Figure 14.1C). Looking at the cumulative score, i.e., the sum of all daily disease scores, HEK and even more so YB2/0 glycovariants exacerbated disease course overall (Figure 14.1D).

Chapter 15

Neuropathological evaluation

After these experiments and analysis of clinical signs, some animals were sacrificed at various timepoints after treatment and fixed using whole-animals perfusion with paraformaldehyde before being shipped to Vienna where we performed neuropathological evaluation.

15.1 Demyelination

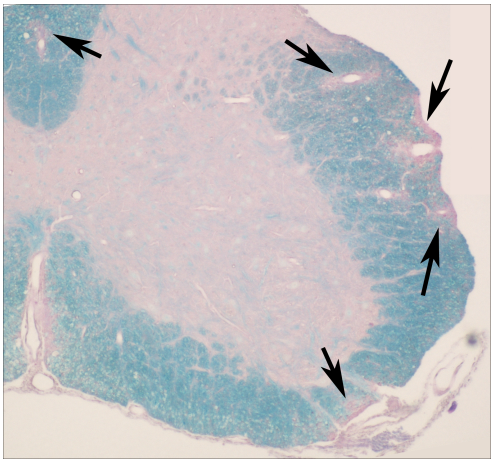

Figure 15.1: The LFB-PAS stain visualizes the pink PAS^+ demyelinated white matter. Demyelination primarily occurs around inflamed blood vessels, as immune cells migrate from the perivascular space into the spinal cord parenchyma.

Animals were sacrificed on Day 12 (d12) or Day 16 (d16) after EAE induction. Animals with EAE develop demyelination in the spinal cord. The extent of demyelination can be shown by staining for LFB-PAS. Areas with intact myelin appear blue, while the debris of myelin destroyed by macrophages becomes PAS^+, making them appear pink. In all animals, demyelination was strongest in the spinal cord. The extent of demyelination was defined as a percentage of spinal cord white matter after measuring the number of blue and pink areas using a 10x10 grid at 2.5x magnification.

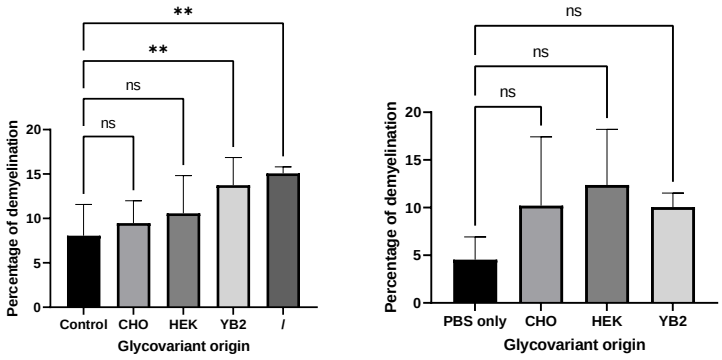

(a) d12 mice **(b)** d16 mice

Figure 15.2: Among d12 mice, those treated with YB2/0 glycovariants and early-onset d12 mice showed increased demyelination, while d16 mice showed signs of recovery, with receding significances and less demyelination overall.

d12 mice with early disease onset showed the greatest extent of demyelination compared to controls despite the absence of any exogenous glycovariants (Figure 15.2a). Among other d12 animals, mice treated with glycovariants originating from YB2/0 cells, i.e., those expressing a high degree of afucosylation, showed significantly more advanced progressions of demyelination compared to controls. d16 animals did not exhibit differences in demarcation of spinal cord white matter (Figure 15.2b) and compared to d12 mice exhibited less demyelination overall.

15.2 Inflammatory index

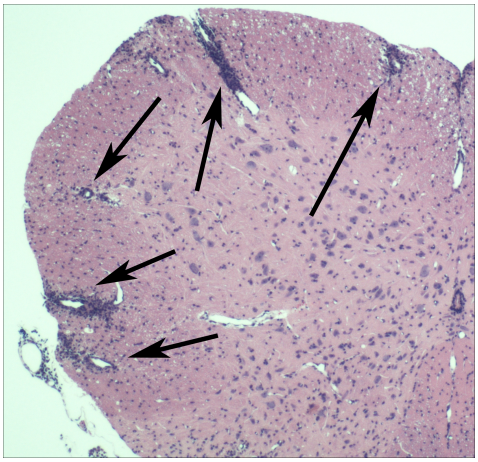

Figure 15.3: Perivascular cuffs surrounding inflamed blood vessels in the spinal cord visualized in an HE stain.

The inflammatory index is defined as the average number of inflamed blood vessels per spinal cord cross section. As such, it is a rough measurement of the degree of inflammation in the spinal cord. The inflammatory cells involved are predominantly constituted by lymphocytes and macrophages, which stain much darker than their surroundings in HE stains;

granulocytes are typically seen at the earliest time points (about one to two days before clinical signs appear).

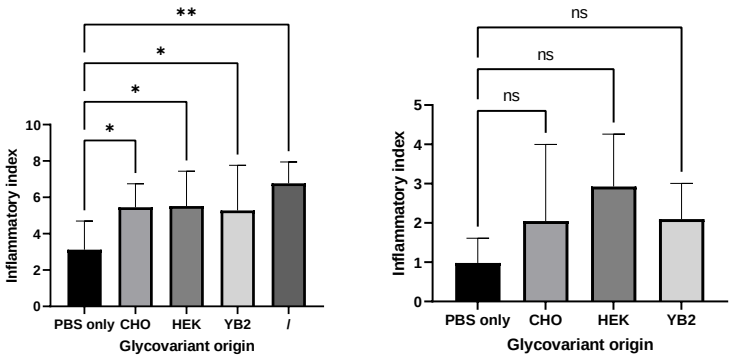

(a) d12 mice **(b)** d16 mice

Figure 15.4: In d12 mice, inflammatory index was increased after glycovariant treatment with early-onset mice exhibiting the highest value. d16 mice, on the other hand, showed no differences between test groups and controls, with lower inflammatory indices overall.

Among all d12 animals, there was an increase in the number of perivascular cuffs in both all groups treated with exogenous glycovariants and early-onset mice compared to controls (Figure 15.4a); however, in contrast to the demyelination experiment, early-onset mice showed diminished significance compared to HEK and YB2/0 mice. By Day 16 there were no significant differences in inflammatory indices of the different groups (Figure 15.4b). Overall, the inflammatory index was diminished compared to d12 mice.

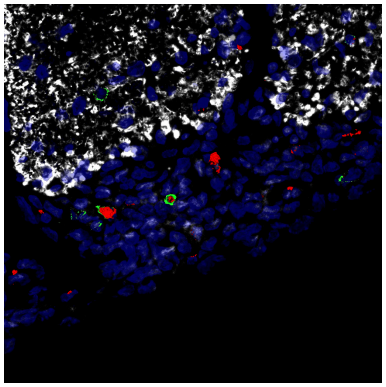

Figure 15.5: PLP (white), CD8a (green), Granzyme B (red), DAPI (blue). Areas with little signal of PLP represent sites of demyelination. $CD8a^{+}GrB^{+}$ cells include NK and NKT cells as well as CTLs, Notably, there are some cells exclusively positive for the Granzyme B marker, which could mean that the antibody binds to other granzymes, non-specificly. The counter-stain for DAPI shows a large accumulation of cells in the site of myelination, which might include various immune cells responsible for the destruction of myelin and/or the removal of its debris in the area.

15.3 T lymphocytes

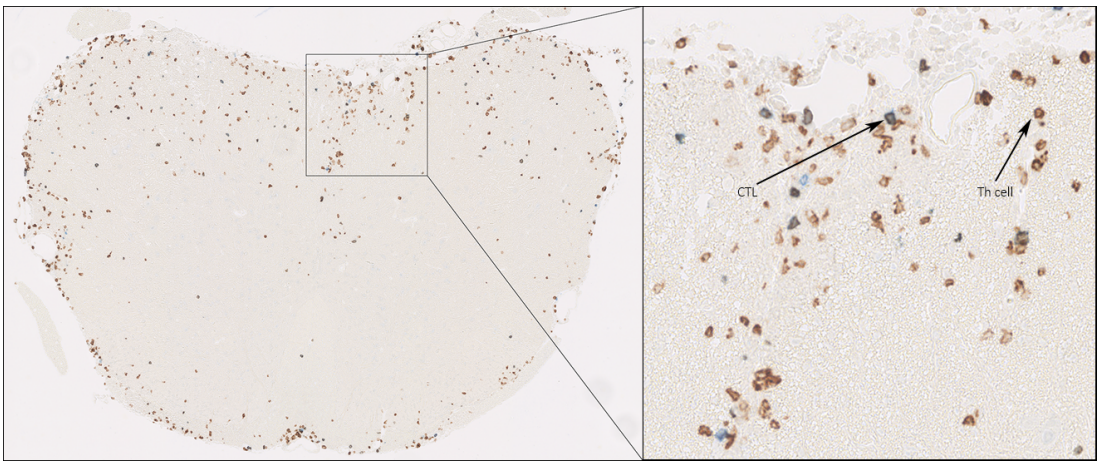

Figure 15.6: CD3 (brown), CD8a (blue). Th cells ($CD3^+CD8a^-$) represent the vast majority of T cells invading the spinal cord parenchyma and perivascular space in EAE. CTLs ($CD3^+CD8a^+$) make up most of the other cells visible in this stain. $CD3^-CD8a^+$ cells could be a number of different cell types, such as NK cells.

MOG_{35-55}-induced EAE in mice elicits a strong T cell response in the CNS. They penetrate the BBB, opening it for other immune cells to follow and participate in cell-mediated immunity.

15.3.1 T cells

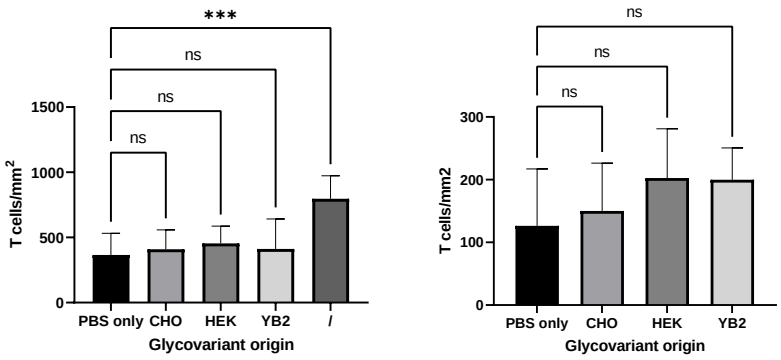

(a) d12 mice **(b)** d16 mice

Figure 15.7: Among d12 mice, only early-onset mice exhibited a significant increase in T cell count compared to controls. d16 mice exhibited a strong decrease overall.

In d12 mice, T cells ($CD3^+$) were spread throughout the entire spinal cord white matter with some local accumulations near blood vessel; however, glycovariants did not appear to affect their number or distribution (Figure 15.7a). Only early-onset mice showed significant increase in T cells compared to controls. Analogous to d12 mice, T cell count in the spinal

cords of d16 mice was not affected by glycovariants (Figure 15.7b). d16 mice also showed an overall lower abundance of T cells compared to d12 mice.

15.3.2 Predominance of $CD4^+$ helper T cells

MOG_{35-55}-EAE is predominantly $CD4^+$ T cell-mediated, with Th cells constituting the vast majority of T cells present in the spinal cord parenchyma and perivascular space of diseased mice (Miller & Karpus, 2007). The overall number of T cells was not affected by the glycovariants; therefore, we tested for changes in the ratio between Th cells ($CD3^+CD8^-$) and other T cells such as NKT cells and CTLs ($CD3^+CD8^+$).

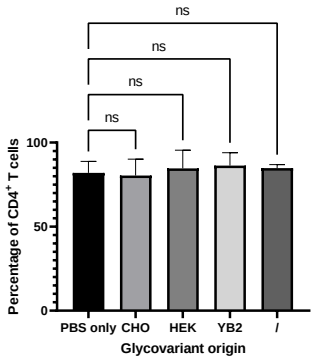

Figure 15.8: The percentage of $CD4^+$ (i.e., $CD8^-$) T cells showed to be affected by neither the exogenous glycovariants, nor early disease-onset in d12 mice.

$CD4^+$ T cells represented the by far most abundant type of lymphocytes to invade the spinal cords' parenchyma in all d12 groups (Figure 15.8). However, we could not show that glycovariants affected their number or predominance among T cells.

15.4 B cells

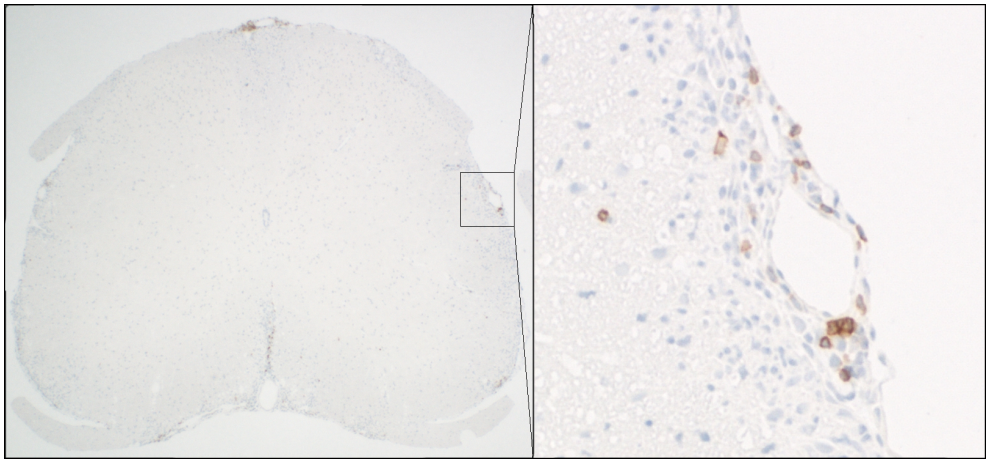

Figure 15.9: B cells (brown) almost exclusively remained in the perivascular space upon MOG_{35-55}-immunization and subsequent injection with glycovariants or PBS only, increasing in number over time.

Aside from T cells we also analyzed B cell infiltration of the spinal cord. We stained for B cells using the marker B220. B cells rarely entered the spinal cord parenchyma themselves but mostly remained within the meninges instead.

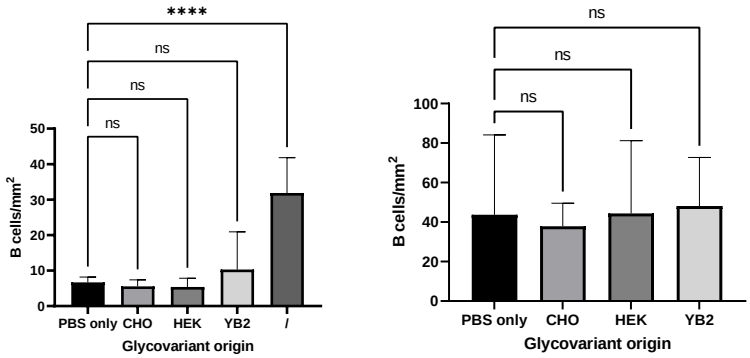

(a) d12 mice **(b)** d16 mice

Figure 15.10: B cell count per mm^2 in the spinal cord's parenchyma, perivascular space, and surrounding meninges only showed to be dependent on time without any changes among mice treated with glycovariants.

On Day 12, B cell count in the spinal cord parenchyma, perivascular space, and surrounding meninges did not significantly change when comparing test groups to controls (Figure 15.10a). Early-onset mice represented the only exception as they exhibited an increased number of B cells. B cell presence was overall increased in d16 mice (Figure 15.10b) compared to d12 mice with no significant differences between groups.

15.5 NK & NKT cells

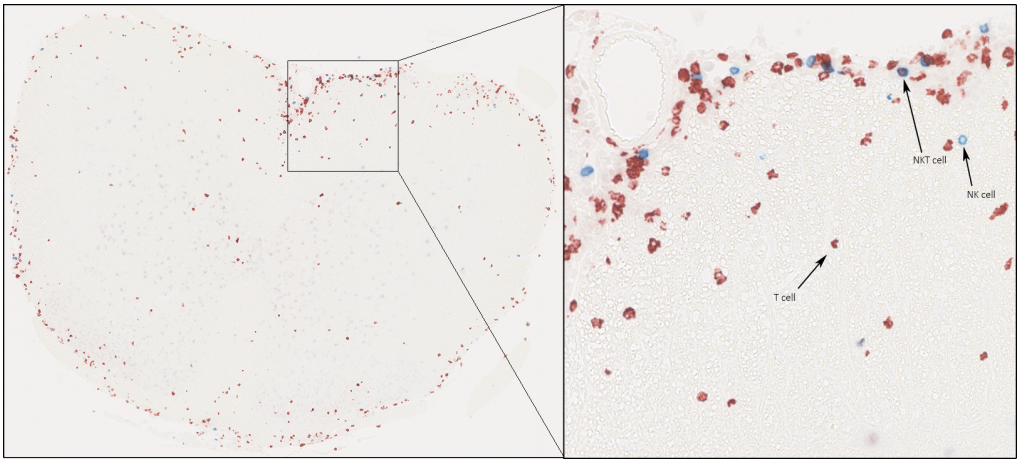

Figure 15.11: CD3 (brown), CD161c (blue). $CD161c^{+}CD3^{-}$ NK cells and $CD161c^{+}CD3^{+}$ NKT cells remained scarce compared to T cells across all test groups, with NK cells being more numerous compared to NKT cells.

15.5.1 $CD161c^{+}$ NK cells/mm^2

NK cells play an important role in immune response. They invade the parenchyma and aid by proinflammatory signaling and ADCC after binding to infected cells or – more specifically – to the antibodies attached to them (Irvine & Alter, 2020). Using the surface receptor CD161c as marker, cross sections were stained for NK cells.

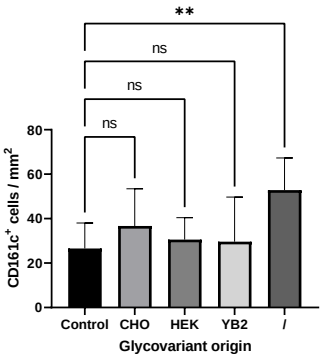

Figure 15.12: In d12 mice $CD161c^{+}$ NK cell count remained unaffected by injection with glycovariants.

d12 mice injected with glycovariants did not exhibit a significant change in the number of NK cells in the spinal cord parenchyma; early-onset mice, on the other hand, appeared to have increased NK cell presence (Figure 15.12).

15.5.2 Percentage of NKT cells among NK cells

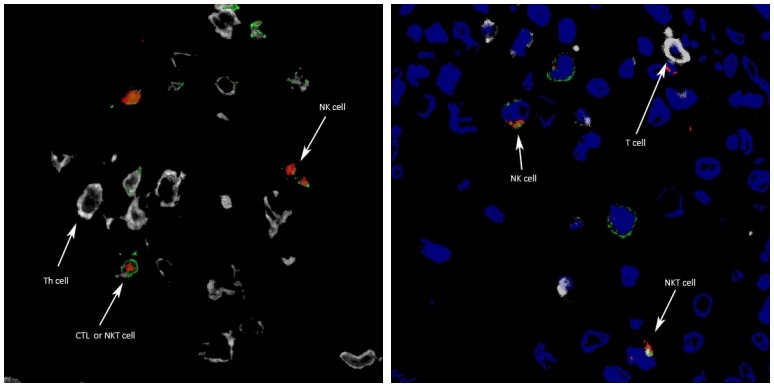

(a) CD3 (w)/CD8a (g)/GrB (r) **(b)** CD3 (w)/CD161c (g)/GrB (r)

Figure 15.13: Both NK and NKT cells are positive for Granzyme B, a serine protease residing in granules in the cytosol of these cells; however, this protein can also be found in CTLs, making it an insufficient marker for NK cells on its own. Even in combination with CD3 and CD8a, it cannot be used to distinguish CTLs from NKT cells. CD3/CD161c/GrB allows a clear differentiation between T cells, NK cells, and NKT cells.

A small subset of NK cells also exhibits T cell features, including the typical surface receptor CD3. Since NK cell count seemed unaffected by the glycovariants, we wanted to ensure that there were no changes within the cell population that could have promoted the increased immune activity indicated by the inflammatory index, either.

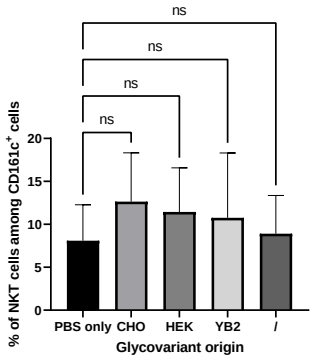

Figure 15.14: The percentage of NKT cells among $CD161c^+$ cells did not change upon treatment with glycovariants in d12 mice.

Neither d12 mice treated with glycovariants, nor those with early disease onset showed any significant changes in the prevalence of NKT cells ($CD161c^+CD3^+$) among all $CD161c^+$ cells (i.e., NK and NKT cells) compared to controls (Figure 15.14).

Part IV

Discussion & outlook

Discussion

Our results show that treatment with anti-MOG IgG_1 glycovariants originating from YB2/0 cells, i.e., those expressing the highest degree of afucosylation, exacerbates symptoms, disease course, demyelination, and inflammatory index in C57BI/6 mice with active anti-MOG EAE. It is important to note, that early-onset mice first exhibited symptoms at various different timepoints, making them unfit as a proper test group; however, their evaluation was still considered as an indicator of what might be happening between Days 12 and 16. We could also show that time and recovery played a major factor, as d12 mice showed more prominent demyelination and inflammatory indices overall compared to those sacrificed on d16. Additionally, unlike d16 mice d12 mice treated with HEK and YB2/0 glycovariants exhibited an increase in demyelination and all d12 mice treated with glycovariants showed prominent inflammatory indices compared to controls. Early-onset d12 mice had an increase in both parameters as well, which suggests that in terms of time the peak might be somewhere in between Days 12 and 16. On Day 16, all significances had receded with no major differences between the individual groups but clear signs of recovery overall. The only exception to this rule was B cell presence which continuously increased over time. T cell and NK cell presence was unaffected by glycovariants with only time span between disease onset and sacrifice playing a factor. There was no change in ratios between different subpopulations we tested for within these cell types at any point in time.

We know that Fc glycosylation is a mechanism allowing for the regulation of antibody function. Fc glycosylation dynamically changes during infection to adapt to the pathogens involved. In healthy individuals, 90% of IgG is core fucosylated in the Fc region, and increased afucosylation has been associated with a fifty-fold increase in affinity for FcγRIIIα, which is prominently expressed on NK cells. Therefore, core afucosylation is strongly associated with enhanced ADCC (Irvine & Alter, 2020). When Dr. Lennart Mars at the Lille Neuroscience & Cognition Institute examined samples from two MOGAD patients, he found that their MOG-specific IgG_1 antibodies were lacking fucose on all glycan moieties. Afucosylation was detectable among 52% and 60% of total serum IgG, respectively, and 98% and 95% of MOG-specific antibodies, respectively. MS patients, on the other hand, usually do not show this abnormal structure to such a high degree; while their IgG typically exhibits increased bisecting GlcNAc associated with reduction in Fc-fucosylation and Fc-galactosylation, the large majority of IgG remains fucosylated (Decker et al., 2016; Wuhrer et al., 2015; Mars, 2020; Irvine & Alter, 2020).

Clinical experiments showed that afucosylated IgG glycovariants had a negative effect on disease course and prognosis of MOG_{35-55}-mice. Glycovariants – both those originating from HEK cells and even more so those from YB2/0 cells – were shown to increase maximal clinical score and cumulative score. Similarly, recovery and survival rate were also strongly diminished following immunization with YB2/0 glycovariants.

Demyelination progressed the farthest in d12 animals that became ill before Day 9 and those who were treated with YB2/0 glycovariants; the latter is consistent with clinical score. d16 mice already showed signs of remission with a decrease in demyelination compared to d12 mice. The inflammatory index showed a clear increase in perivascular cuffs for all three d12 test groups. The inflammatory index in d16 mice showed no differences compared to controls and was lower overall compared to d12 mice treated with glycovariants.

Interestingly, early-onset mice's inflammatory index was less significantly increased than

their T cell count, which could mean that the influx of new immune cells through the opened BBB had already subsided at the day of sacrifice, while already present immune cells had migrated into the parenchyma where they continued to damage the white matter tissue, explaining the increase in demyelination and T cell presence. This is further supported by d16 animals, where inflammatory indices and T cell presence were even more decreased across all groups compared to d12 mice treated with glycovariants. Total T cell count was unaffected in all d12 and d16 mice compared to controls, but we did not test for how many of them were specific T cells to epitopes present in the spinal cord and what fraction was constituted by non-specific T cells entering the parenchyma and perivascular space as a result of the bystander effect (Whiteside et al., 2018). The ratio between $CD4^+$ and $CD8^+$ T cells in the spinal cord parenchyma did not change at any point between any of the test groups, either.

There was no correlation between B cell count and demyelination, inflammatory index, or T cell count. As expected, active EAE induced by immunization with $MOG_{35\text{-}55}$ hardly caused a B cell-mediated response (Sato et al., 2018). However, B cell presence did eventually increase after an extended delay, with d16 mice exhibiting heightened B cell presence in the spinal cord parenchyma and perivascular space. This could be the result of macrophages presenting MOG and other brain-derived protein fragments on their surfaces escaping the inflammatory lesions in the spinal cord. Similarly, d12 early-onset mice showed a significantly higher B cell count compared to controls; however, to reiterate, these mice cannot be used as a proper test group due to their different disease onset time points.

We could not show that increased affinity of intravenously injected afucosylated IgGs for FcγRIIIα (Irvine & Alter, 2020) amplifies NK cell recruitment in the spinal cord parenchyma, at least in case of $CD161c^+$ NK cells. The number of NK cells remained minimal and unchanged compared to other $CD8^+$ lymphocytes. There were also no changes in ratio between NK and NKT cells that could have indicated an influence on the immune response. As such, from our findings it is not clear what processes predominantly contributed to inflammatory index and demyelination. Other mechanisms might have been responsible for attracting immune cells from the periphery. For example, microglia and inflamed endothelia are competent in recruiting macrophages and T cells constituting a large portion of cells in the perivascular cuffs (Leach et al., 2013; Rao et al., 2007). A previous study has also implicated the complement system as the dominant (if not only) effector cascade invoked by demyelinating Abs in both MS and EAE, making it a likely cause for the exacerbation of symptoms and neuropathology; on the contrary, the authors could not establish any involvement of ADCC in the autoantibody-mediated tissue damage (Urich et al., 2006). However, there is no literature connecting afucosylation of IgG with increased complement activation. Instead, it is Fc-galactosylation that has been shown to greatly enhance complement activation (Reusch & Tejada, 2015; van der Horst et al., 2020; van Osch et al., 2021; Peschke et al., 2017). Hence, the question arises how YB2/0 glycovariants were the only immunoglobulins consistently affecting clinical scores and neuropathology, especially when considering that 8-18C5 IgG_1 is designed to initially induce complement-mediated demyelination by default; afucosylated IgG is normally galactosylated at about the same rate as fucosylated IgG (Dekkers et al., 2018). Autoantibodies are still involved in the recruitment of FcR-bearing cells such as NK cells, and afucosylated glycovariants could amplify this effect on NK cells even further (Irvine & Alter, 2020); however, glycovariants were injected into the bloodstream, not the CNS. As such, interaction between NK cells and glycovariants might have predominantly taken place within the secondary lymphoid organs, such as the spleen.

Outlook

To determine whether NK/NKT cell count in the spinal cord parenchyma and perivascular space is truly unaffected by glycovariant injection, alternative markers for NK cells or combinations thereof should be employed; a promising candidate is NKp46 (also called CD335), a universal marker for NK cells in mammals (Westgaard et al., 2004). Additionally, considering the findings by Urich et al. in 2006 the involvement of the complement system should be explored and the localization of complement plaques compared with the localization of inflammatory lesions; a stain for C1q, a product of the classical complement pathway, would be most appropriate, given that this pathway is invoked by IgG presence (Ingram et al., 2014; Urich et al., 2006).

List of Figures

List of Tables

Bibliography

Abbas, A. K., Lichtman, A. H., Pillai, S., & Abbas, A. K. (2018). *Cellular and Molecular Immunology*. Elsevier.

Ambrosius, W., Michalak, S., Kozubski, W., & Kalinowska, A. (2020). Myelin Oligodendrocyte Glycoprotein Antibody-Associated Disease: Current Insights into the Disease Pathophysiology, Diagnosis and Management. *International Journal of Molecular Sciences*, 22(1), 100.

Andoh, M., Ikegaya, Y., & Koyama, R. (2019). Synaptic Pruning by Microglia in Epilepsy. *Journal of clinical medicine*, 8(12).

Banks, W. A. (2009). Characteristics of compounds that cross the blood-brain barrier. *BMC neurology*, 9 Suppl 1, S3.

Baumgärtner, W. & Alldinger, S. (2005). The pathogenesis of canine distemper virus induced demyelination. In E. Lavi & C. S. Constantinescu (Eds.), *Experimental Models of Multiple Sclerosis* (pp. 871–887). Boston, MA: Springer US.

Brandstadter, R. & Katz Sand, I. (2017). The use of natalizumab for multiple sclerosis. *Neuropsychiatric Disease and Treatment*, Volume 13, 1691–1702.

Breithaupt, C., Schubart, A., Zander, H., Skerra, A., Huber, R., Linington, C., & Jacob, U. (2003). Structural insights into the antigenicity of myelin oligodendrocyte glycoprotein. *Proceedings of the National Academy of Sciences*, 100(16), 9446–9451.

Chastain, E. M. L., Duncan, D. S., Rodgers, J. M., & Miller, S. D. (2011). The role of antigen presenting cells in multiple sclerosis. *Biochimica et biophysica acta*, 1812(2), 265–274.

Chen, J. J., Flanagan, E. P., Jitprapaikulsan, J., López-Chiriboga, A. S. S., Fryer, J. P., Leavitt, J. A., Weinshenker, B. G., McKeon, A., Tillema, J.-M., Lennon, V. A., Tobin, W. O., Keegan, B. M., Lucchinetti, C. F., Kantarci, O. H., McClelland, C. M., Lee, M. S., Bennett, J. L., Pelak, V. S., Chen, Y., VanStavern, G., Adesina, O.-O. O., Eggenberger, E. R., Acierno, M. D., Wingerchuk, D. M., Brazis, P. W., Sagen, J., & Pittock, S. J. (2018). Myelin Oligodendrocyte Glycoprotein Antibody–Positive Optic Neuritis: Clinical Characteristics, Radiologic Clues, and Outcome. *American Journal of Ophthalmology*, 195, 8–15.

Coggan, J., Bittner, S., Stiefel, K., Meuth, S., & Prescott, S. (2015). Physiological Dynamics in Demyelinating Diseases: Unraveling Complex Relationships through Computer Modeling. *International Journal of Molecular Sciences*, 16(9), 21215–21236.

Constantinescu, C. S., Hilliard, B., Ventura, E., Wysocka, M., Showe, L., Lavi, E., Fujioka, T., Scott, P., Trinchieri, G., & Rostami, A. (2001). Modulation of susceptibility and resistance to an autoimmune model of multiple sclerosis in prototypically susceptible and resistant strains by neutralization of interleukin-12 and interleukin-4, respectively. *Clinical Immunology*, 98(1), 23–30.

Cooper, M. A., Elliott, J. M., Keyel, P. A., Yang, L., Carrero, J. A., & Yokoyama, W. M. (2009). Cytokine-induced memory-like natural killer cells. *Proceedings of the National Academy of Sciences of the United States of America*, 106(6), 1915–1919.

Daneman, R. & Prat, A. (2015). The blood-brain barrier. *Cold Spring Harbor Perspectives in Biology*, 7(1), a020412.

Decker, Y., Schomburg, R., Németh, E., Vitkin, A., Fousse, M., Liu, Y., & Fassbender, K. (2016). Abnormal galactosylation of immunoglobulin G in cerebrospinal fluid of multiple sclerosis patients. *Multiple Sclerosis Journal*, 22(14), 1794–1803.

Dekkers, G., Rispens, T., & Vidarsson, G. (2018). Novel Concepts of Altered Immunoglobulin G Galactosylation in Autoimmune Diseases. *Frontiers in Immunology*, 9, 553.

Dokun, A. O., Kim, S., Smith, H. R., Kang, H. S., Chu, D. T., & Yokoyama, W. M. (2001). Specific and nonspecific NK cell activation during virus infection. *Nature immunology*, 2(10), 951–956.

Dutta, S. S. (2018). Types of Antibodies. https://www.news-medical.net/life-sciences/Types-of-Antibodies.aspx.

Efendi, H. (2016). Clinically Isolated Syndromes: Clinical Characteristics, Differential Diagnosis, and Management. *Noro Psikiyatri Arsivi*, 52(Suppl.1), 1–11.

Eissmann, P. (2021). Natural Killer Cells. https://www.immunology.org/public-information/bitesized-immunology/cells/natural-killer-cells.

El-Khoury, N., Braun, A., Hu, F., Pandey, M., Nedergaard, M., Lagamma, E. F., & Ballabh, P. (2006). Astrocyte end-feet in germinal matrix, cerebral cortex, and white matter in developing infants. *Pediatric research*, 59(5), 673–679.

Engelhardt, B. & Ransohoff, R. M. (2012). Capture, crawl, cross: The T cell code to breach the blood–brain barriers. *Trends in Immunology*, 33(12), 579–589.

Fernando, V., Omura, S., Sato, F., Kawai, E., Martinez, N. E., Elliott, S. F., Yoh, K., Takahashi, S., & Tsunoda, I. (2014). Regulation of an autoimmune model for multiple sclerosis in th2-biased GATA3 transgenic mice. *International Journal of Molecular Sciences*, 15(2), 1700–1718.

Flach, A.-C., Litke, T., Strauss, J., Haberl, M., Gómez, C. C., Reindl, M., Saiz, A., Fehling, H.-J., Wienands, J., Odoardi, F., Lühder, F., & Flügel, A. (2016). Autoantibody-boosted T-cell reactivation in the target organ triggers manifestation of autoimmune CNS disease. *Proceedings of the National Academy of Sciences*, 113(12), 3323–3328.

Friese, M. A., Montalban, X., Willcox, N., Bell, J. I., Martin, R., & Fugger, L. (2006). The value of animal models for drug development in multiple sclerosis. *Brain : a journal of neurology*, 129(Pt 8), 1940–1952.

Goldmann, T. & Prinz, M. (2013). Role of microglia in CNS autoimmunity. *Clinical & developmental immunology*, 2013, 208093.

Gomes, C., Ferreira, R., George, J., Sanches, R., Rodrigues, D. I., Gonçalves, N., & Cunha, R. A. (2013). Activation of microglial cells triggers a release of brain-derived neurotrophic factor (BDNF) inducing their proliferation in an adenosine A2A receptor-dependent manner: A2A receptor blockade prevents BDNF release and proliferation of microglia. *Journal of Neuroinflammation*, 10(1), 780.

Goverman, J. (2009). Autoimmune T cell responses in the central nervous system. *Nature Reviews Immunology*, 9(6), 393–407.

Grider, M. H., Belcea, C. Q., Covington, B. P., Reddy, V., & Sharma, S. (2021). Neuroanatomy, Nodes of Ranvier. In *StatPearls*. Treasure Island (FL): StatPearls Publishing.

Gudelj, I., Lauc, G., & Pezer, M. (2018). Immunoglobulin G glycosylation in aging and diseases. *Cellular Immunology*, 333, 65–79.

Hanlon, K. E. & Vanderah, T. W. (2010). Chapter one - constitutive activity at the cannabinoid CB1 receptor and behavioral responses. In P. M. Conn (Ed.), *Constitutive Activity in Receptors and Other Proteins, Part a*, volume 484 of *Methods in Enzymology* (pp. 3–30). Academic Press.

Hickey, W. F. (2001). Basic principles of immunological surveillance of the normal central nervous system. *Glia*, 36(2), 118–124.

Hohl, T. M. (2015). 6 - cell-mediated defense against infection. In J. E. Bennett, R. Dolin, & M. J. Blaser (Eds.), *Mandell, Douglas, and Bennett's Principles and Practice of Infectious Diseases (Eighth Edition)* (pp. 50–69.e6). Philadelphia: W.B. Saunders, eighth edition edition.

Hor, J. Y., Asgari, N., Nakashima, I., Broadley, S. A., Leite, M. I., Kissani, N., Jacob, A., Marignier, R., Weinshenker, B. G., Paul, F., Pittock, S. J., Palace, J., Wingerchuk, D. M., Behne, J. M., Yeaman, M. R., & Fujihara, K. (2020). Epidemiology of Neuromyelitis Optica Spectrum Disorder and Its Prevalence and Incidence Worldwide. *Frontiers in Neurology*, 11, 501.

Ingram, G., Loveless, S., Howell, O. W., Hakobyan, S., Dancey, B., Harris, C. L., Robertson, N. P., Neal, J. W., & Morgan, B. P. (2014). Complement activation in multiple sclerosis plaques: An immunohistochemical analysis. *Acta Neuropathologica Communications*, 2(1), 53.

Irvine, E. B. & Alter, G. (2020). Understanding the role of antibody glycosylation through the lens of severe viral and bacterial diseases. *Glycobiology*, 30(4), 241–253.

Jäger, A., Dardalhon, V., Sobel, R. A., Bettelli, E., & Kuchroo, V. K. (2009). Th1, Th17, and Th9 Effector Cells Induce Experimental Autoimmune Encephalomyelitis with Different Pathological Phenotypes. *The Journal of Immunology*, 183(11), 7169.

Janeway, C., Ed. (2001). *Immunobiology: The Immune System in Health and Disease ; [Animated CD-ROM Inside]*. New York, NY: Garland Publ. [u.a.], 5. ed edition.

Jennewein, M. F. & Alter, G. (2017). The Immunoregulatory Roles of Antibody Glycosylation. *Trends in Immunology*, 38(5), 358–372.

Kale, N. (2016). Optic neuritis as an early sign of multiple sclerosis. *Eye and Brain*, Volume 8, 195–202.

Kohm, A. P., Carpentier, P. A., Anger, H. A., & Miller, S. D. (2002). Cutting Edge: $CD4^+CD25^+$ Regulatory T Cells Suppress Antigen-Specific Autoreactive Immune Responses and Central Nervous System Inflammation During Active Experimental Autoimmune Encephalomyelitis. *The Journal of Immunology*, 169(9), 4712.

Kubotera, H., Ikeshima-Kataoka, H., Hatashita, Y., Allegra Mascaro, A. L., Pavone, F. S., & Inoue, T. (2019). Astrocytic endfeet re-cover blood vessels after removal by laser ablation. *Scientific Reports*, 9(1), 1263.

Kuchroo, V. K., Prabhu Das, M., Brown, J. A., Ranger, A. M., Zamvil, S. S., Sobel, R. A., Weiner, H. L., Nabavi, N., & Glimcher, L. H. (1995). B7-1 and B7-2 costimulatory molecules activate differentially the Th1/Th2 developmental pathways: Application to autoimmune disease therapy. *Cell*, 80(5), 707–718.

Kumar, A., Suryadevara, N., Hill, T. M., Bezbradica, J. S., Van Kaer, L., & Joyce, S. (2017). Natural killer t cells: An ecological evolutionary developmental biology perspective. *Frontiers in Immunology*, 8, 1858.

Lassmann, H. (2020). Pathology of inflammatory diseases of the nervous system: Human disease versus animal models. *Glia*, 68(4), 830–844.

Lassmann, H., Brück, W., & Lucchinetti, C. (2001). Heterogeneity of multiple sclerosis pathogenesis: Implications for diagnosis and therapy. *Trends in molecular medicine*, 7(3), 115–121.

Leach, H. G., Chrobak, I., Han, R., & Trojanowska, M. (2013). Endothelial Cells Recruit Macrophages and Contribute to a Fibrotic Milieu in Bleomycin Lung Injury. *American Journal of Respiratory Cell and Molecular Biology*, 49(6), 1093–1101.

Li, J., Yin, W., Jing, Y., Kang, D., Yang, L., Cheng, J., Yu, Z., Peng, Z., Li, X., Wen, Y., Sun, X., Ren, B., & Liu, C. (2019). The Coordination Between B Cell Receptor Signaling and the Actin Cytoskeleton During B Cell Activation. *Frontiers in Immunology*, 9, 3096.

Mannara, F., Valente, T., Saura, J., Graus, F., Saiz, A., & Moreno, B. (2012). Passive experimental autoimmune encephalomyelitis in C57BL/6 with MOG: Evidence of involvement of B cells. *PloS one*, 7(12), e52361.

Mars, L. (2020). Project proposal to Fondation ARSEP - Effects of Fc-glycosylation of autoantibodies in demyelinating diseases.

Mars, L. T., Saikali, P., Liblau, R. S., & Arbour, N. (2011). Contribution of CD8 T lymphocytes to the immuno-pathogenesis of multiple sclerosis and its animal models. *Biochimica et Biophysica Acta (BBA) - Molecular Basis of Disease*, 1812(2), 151–161.

Matusevicius, D., Kivisäkk, P., He, B., Kostulas, N., Ozenci, V., Fredrikson, S., & Link, H. (1999). Interleukin-17 mRNA expression in blood and CSF mononuclear cells is augmented in multiple sclerosis. *Multiple sclerosis (Houndmills, Basingstoke, England)*, 5(2), 101–104.

McGavern, D. B. (2005). The role of bystander T cells in CNS pathology and pathogen clearance. *Critical Reviews in Immunology*, 25(4), 289–303.

Merrill, J. E., Kagan, J. M., Schmid, I., Strom, S. R., Quan, S. G., & Chen, I. S. (1989). T cell lines established from multiple sclerosis cerebrospinal fluid T cells using human retroviruses. *Journal of Neuroimmunology*, 21(2), 213–226.

Mestas, J. & Hughes, C. C. W. (2004). Of Mice and Not Men: Differences between Mouse and Human Immunology. *The Journal of Immunology*, 172(5), 2731.

Miller, S. D. & Karpus, W. J. (2007). Experimental autoimmune encephalomyelitis in the mouse. *Current protocols in immunology*, Chapter 15, Unit 15.1.

Murphy, K. M. & Weaver, C. (2017). *Janeway's Immunobiology*. New York London: GS, Garland Science, Taylor & Francis Group, 9th edition edition.

Nakato, H. & Li, J.-P. (2016). Chapter seven - functions of heparan sulfate proteoglycans in development: Insights from drosophila models. In K. W. Jeon (Ed.), *International Review of Cell and Molecular Biology*, volume 325 of *International Review of Cell and Molecular Biology* (pp. 275–293). Academic Press.

O'Connor, R. A., Prendergast, C. T., Sabatos, C. A., Lau, C. W. Z., Leech, M. D., Wraith, D. C., & Anderton, S. M. (2008). Cutting Edge: Th1 Cells Facilitate the Entry of Th17 Cells to the Central Nervous System during Experimental Autoimmune Encephalomyelitis. *The Journal of Immunology*, 181(6), 3750.

Opsahl, M. L. (2005). Early and late HHV-6 gene transcripts in multiple sclerosis lesions and normal appearing white matter. *Brain*, 128(3), 516–527.

Ousman, S. S. & Kubes, P. (2012). Immune surveillance in the central nervous system. *Nature Neuroscience*, 15(8), 1096–1101.

Penderis, J., Shields, S. A., & Franklin, R. J. M. (2003). Impaired remyelination and depletion of oligodendrocyte progenitors does not occur following repeated episodes of focal demyelination in the rat central nervous system. *Brain*, 126(6), 1382–1391.

Peschke, B., Keller, C. W., Weber, P., Quast, I., & Lünemann, J. D. (2017). Fc-Galactosylation of Human Immunoglobulin Gamma Isotypes Improves C1q Binding and Enhances Complement-Dependent Cytotoxicity. *Frontiers in Immunology*, 8, 646.

Pfeifle, R., Rothe, T., Ipseiz, N., Scherer, H. U., Culemann, S., Harre, U., Ackermann, J. A., Seefried, M., Kleyer, A., Uderhardt, S., Haugg, B., Hueber, A. J., Daum, P., Heidkamp, G. F., Ge, C., Böhm, S., Lux, A., Schuh, W., Magorivska, I., Nandakumar, K. S., Lönnblom, E., Becker, C., Dudziak, D., Wuhrer, M., Rombouts, Y., Koeleman, C. A., Toes, R., Winkler, T. H., Holmdahl, R., Herrmann, M., Blüml, S., Nimmerjahn, F., Schett, G., & Krönke, G. (2017). Regulation of autoantibody activity by the IL-23-T(H)17 axis determines the onset of autoimmune disease. *Nature immunology*, 18(1), 104–113.

Pierson, E. R., Stromnes, I. M., & Goverman, J. M. (2014). B cells promote induction of experimental autoimmune encephalomyelitis by facilitating reactivation of T cells in the central nervous system. *Journal of immunology (Baltimore, Md. : 1950)*, 192(3), 929–939.

Rao, R. M., Yang, L., Garcia-Cardena, G., & Luscinskas, F. W. (2007). Endothelial-Dependent Mechanisms of Leukocyte Recruitment to the Vascular Wall. *Circulation Research*, 101(3), 234–247.

Rasband, M. N. & Macklin, W. B. (2012). Chapter 10 - myelin structure and biochemistry. In S. T. Brady, G. J. Siegel, R. W. Albers, & D. L. Price (Eds.), *Basic Neurochemistry (Eighth Edition)* (pp. 180–199). New York: Academic Press, eighth edition edition.

Reusch, D. & Tejada, M. L. (2015). Fc glycans of therapeutic antibodies as critical quality attributes. *Glycobiology*, 25(12), 1325–1334.

Roghanian, A. (2021). Dendritic Cells. https://www.immunology.org/public-information/bitesized-immunology/cells/dendritic-cells.

Sato, F., Omura, S., Martinez, N. E., & Tsunoda, I. (2018). Chapter 3 - animal models of multiple sclerosis. In A. Minagar (Ed.), *Neuroinflammation (Second Edition)* (pp. 37–72). Academic Press, second edition edition.

Sawchenko, P. E. (2003). Signaling the brain in systemic inflammation the role of perivascular cells. *Frontiers in Bioscience*, 8(6), s1321–1329.

Schroeder, H. W. J. & Cavacini, L. (2010). Structure and function of immunoglobulins. *The Journal of allergy and clinical immunology*, 125(2 Suppl 2), S41–52.

Schuhmacher, B. (2014). *Analyse von Mikrogliaknötchen in Experimenteller Autimmunenzephalomyelitis*. PhD thesis, Fachhochschule FH Campus Wien.

Semple, B. D., Kossmann, T., & Morganti-Kossmann, M. C. (2010). Role of Chemokines in CNS Health and Pathology: A Focus on the CCL2/CCR2 and CXCL8/CXCR2 Networks. *Journal of Cerebral Blood Flow & Metabolism*, 30(3), 459–473.

Sevenich, L. (2018). Brain-Resident Microglia and Blood-Borne Macrophages Orchestrate Central Nervous System Inflammation in Neurodegenerative Disorders and Brain Cancer. *Frontiers in Immunology*, 9, 697.

Simpson, D. S. A. & Oliver, P. L. (2020). ROS Generation in Microglia: Understanding Oxidative Stress and Inflammation in Neurodegenerative Disease. *Antioxidants*, 9(8), 743.

Stromnes, I. M. & Goverman, J. M. (2006). Active induction of experimental allergic encephalomyelitis. *Nature protocols*, 1(4), 1810–1819.

Tsunoda, I., Libbey, J. E., Kuang, L.-Q., Terry, E. J., & Fujinami, R. S. (2005). Massive apoptosis in lymphoid organs in animal models for primary and secondary progressive multiple sclerosis. *The American Journal of Pathology*, 167(6), 1631–1646.

Urich, E., Gutcher, I., Prinz, M., & Becher, B. (2006). Autoantibody-mediated demyelination depends on complement activation but not activatory Fc-receptors. *Proceedings of the National Academy of Sciences*, 103(49), 18697–18702.

van der Horst, H. J., Nijhof, I. S., Mutis, T., & Chamuleau, M. E. D. (2020). Fc-Engineered Antibodies with Enhanced Fc-Effector Function for the Treatment of B-Cell Malignancies. *Cancers*, 12(10), 3041.

van Osch, T. L. J., Nouta, J., Derksen, N. I. L., van Mierlo, G., van der Schoot, C. E., Wuhrer, M., Rispens, T., & Vidarsson, G. (2021). Fc Galactosylation Promotes Hexamerization of Human IgG1, Leading to Enhanced Classical Complement Activation. *The Journal of Immunology*, 207(6), 1545–1554.

Vivier, E., Raulet, D. H., Moretta, A., Caligiuri, M. A., Zitvogel, L., Lanier, L. L., Yokoyama, W. M., & Ugolini, S. (2011). Innate or adaptive immunity? the example of natural killer cells. *Science (New York, N.Y.)*, 331(6013), 44–49.

Wekerle, H. (2008). Lessons from multiple sclerosis: Models, concepts, observations. *Annals of the rheumatic diseases*, 67 Suppl 3, iii56–60.

Westgaard, I. H., Berg, S. F., Vaage, J. T., Wang, L. L., Yokoyama, W. M., Dissen, E., & Fossum, S. (2004). Rat NKp46 activates natural killer cell cytotoxicity and is associated with FcεRIγ and CD3ζ. *Journal of Leukocyte Biology*, 76(6), 1200–1206.

Whiteside, S. K., Snook, J. P., Williams, M. A., & Weis, J. J. (2018). Bystander T Cells: A Balancing Act of Friends and Foes. *Trends in Immunology*, 39(12), 1021–1035.

Wuhrer, M., Selman, M. H. J., McDonnell, L. A., Kümpfel, T., Derfuss, T., Khademi, M., Olsson, T., Hohlfeld, R., Meinl, E., & Krumbholz, M. (2015). Pro-inflammatory pattern of IgG1 Fc glycosylation in multiple sclerosis cerebrospinal fluid. *Journal of Neuroinflammation*, 12(1), 235.

Wynford-Thomas, R., Jacob, A., & Tomassini, V. (2019). Neurological update: MOG antibody disease. *Journal of Neurology*, 266(5), 1280–1286.

Zheng, Y., Cai, M.-T., Li, E.-C., Fang, W., Shen, C.-H., & Zhang, Y.-X. (2021). Case Report: Myelin Oligodendrocyte Glycoprotein Antibody-Associated Disorder Masquerading as Multiple Sclerosis: An Under-Recognized Entity? *Frontiers in Immunology*, 12, 671425.

Appendix

Appendix A:

Protocols

Protocol for HE Stain

1. Dewax in xylene → 2x15min
2. Rehydrate slides through graded ethanol 96% → 70% → 50% → a.d.
3. 5 min Mayer's Hemalaun (Merck #1.09249)
4. Rinse in H2O (tap water)
5. Differentiate in HCl-ethanol
6. Rinse in H2O (tap water)
7. 5 min Scott's solution
8. Rinse in H2O (tap water)
9. 3 min Eosin
10. Rinse in H2O (tap water)
11. Dehydrate slides through graded ethanol, n-butyl acetate, mount with Eukitt

HCl-ethanol
100ml 70% ethanol
0.5ml conc. HCl (37%)

Scott's solution
2g KHCO3
20g MgSO4 x 7H_2O
1000ml H_2O

Eosin stock solution
10g Eosin yellowish in 100ml a.dest.
Let solution mature some days until it is completely dissolved

Eosin working solution
2.5ml stock + 250ml a.dest.
12 gtt acetic acid

Protocol for LFB-PAS Stain

1. Dewax in xylene → 2x15 min
2. Rinse 2x in 96% ethanol
3. Put slides into 0.1% Luxol Fast Blue in the heater → at 57°C over night
4. Cool down
5. Rinse in 96% ethanol
6. Rinse in a.d.
7. 0.1% aqueous lithium carbonate → 5 min
8. Differentiate slides in 70% ethanol until grey and white matter are clearly distinguishable
9. Rinse in a.d.
   PAS reaction
10. 0.8% periodic acid → 10 Min
11. Rinse in a.d.
12. Schiff's reagent → 20 min
13. 3x sulfite washing solution, 2 min each
14. Rinse in running tap water → 5 min
15. Dehydrate slides through graded ethanol, n-butyl acetate, mount with Eukitt

Luxol Fast Blue:
1g Luxol Fast Blue in 1000ml 96% ethanol (solve over night at 57°C)

Periodic acid
4g periodic acid
500ml a.d.

Sulfite washing solution
500ml a.d.
5ml conc.HCl (37%)
20ml 10% potassium- or sodium metabisulfite (in a.d.)

Standard Protocol for IHC Stain with DAB

1. Dewax in Xylene → 2x15min
2. Rinse in 2 changes of 96% ethanol
3. Block the endogenous peroxidase: with 0.2% H2O2 (30%)/ Methanol → 30min
4. Rinse in the second 96% ethanol
5. Rehydrate the slides through graded ethanol 70% → 50% → a.d.
6. Pretreatment if necessary (HIER)
7. Rinse in TBS 3-5x
8. Block non-specific background reactions with 10% FCS/ DAKO-buffer → 15 min
9. Primary antibody diluted in 10%FCS/ DAKO → 4°C over night
10. Rinse in TBS 3-5x
11. Biotinylated secondary antibody in 10% FCS/ DAKO → 1h room temperature
12. Rinse in TBS 3-5x
13. Avidin-Peroxidase 1:500 in 10% FCS/ DAKO → 1h room temperature
14. Rinse in TBS 3-5x
15. Develop with DAB
16. Stop the reaction with tap water or TBS
17. Enhance staining signal with copper sulfate or 0.2% osmium on demand
18. Counterstain with for Hemalaun 20 sec, rinse with tap water
19. Differentiate the slides in HCl-ethanol for a few seconds
20. Scott solution →5 min
21. Dehydrate slides through graded ethanol, n-Butyl acetate
22. Mount slides with Eukitt

NOTE: All incubation steps must be done in a wet chamber – the slides must not dry out during the procedure.

Protocol for HIER

1. Place slides in a plastic char filled with Tris-EDTA or citrate buffer
2. Put the char into a household vegetable steamer for 1 h
3. Remove the char from steamer and let the slides cool down at room temperature for at least 15 minutes
4. Rinse the sections in TBS

Citrate-buffer pH 6,0

2.10g citric acid in 1L a.d.

EDTA buffer

20x stock solution
50ml a. bidest
1.21g TRIS (10mM)
0.37g EDTA (1mM)
→ Adjust pH to 8.5

Working solution
2.5ml stock solution in 50ml a.bidest.

Protocol for CSA

Preparation

1. Borate Buffer: 0.1545g boric acid (Merck # 1.00165) in 50ml dist. water, adjust to pH 8.0 with NaOH
2. 6ml borate buffer + 15mg sulpho-NHS-LCS-Biotin (Pierce, P.O.B. 117, Illinois, 61105, USA – No. 21335)
3. Add 4.5 mg tyramine (Sigma T-7255)
4. Stir overnight at room temperature
5. Filter (0.45 µm)
6. Make small aliquots (10-20µl), store at –20°C

Application

1. Perform immunostaining according to routine protocol until the step with avidin-peroxidase
2. Biotinylated tyramine in PBS containing H_2O_2 30% 1:1000 – optimal working dilution must be determined by end user – we usually apply CSA 20min at room temperature
3. PBS rinse
4. Apply an avidin/streptavidin bound to peroxidase/alkaline phosphatase/fluorescent dye →30min at room temperature
5. TBS rinse
6. Develop with DAB or AEC, counterstain, and mount as usual

DAKO buffer: commercial buffer solution from Dako corporation, 10x (#S3006)
FCS = Fetal Calf Serum

Protocol for Fast Blue

1. Prewarm glassware at 37°C
2. Store buffer at 37°C
3. Staining is done at 37°C under microscopical control (10-45 min)

Stock solution

1. Tris-HCl-buffer 0,1M pH 8,5 – store at 37°C
   12.1g Tris in 1L a.d.
   Adjust pH with HCl
2. 4% NaNO2 (sodium nitrite) – not older than 2 weeks
   0.4g NaNO2 in 10ml a.d.
3. 1M Levamisole in Tris-HCL buffer
   2.408g Levamisole in 10ml TRIS-HCl-buffer
   → Aliquot in 1ml, store at -20°C

50ml working solution

1. Solve 0.00625g naphthol-AS-MX-phosphate in 308µl dimethylformamide
2. Mix it with 50ml warm Tris-HCl-buffer
3. Mix 0.0125g Fast Blue BB Salt with 3085µl 2N HCl (it does not dissolve)
4. Add 308µl NaNO2, shake it 1 min, add mixture to 50ml Tris-HCl-buffer
5. Add 77µl 1M Levamisole, short incubation
6. Filter it
7. Develop the slides at 37°C under microscopical control (10-45min)

Protocol for Fast Red

1. Rinse slide with water
2. Apply staining solution
3. Reaction is done at 4°C, possibly also overnight

Stock solution/APAAP (alkaline phosphatase anti-alkaline phosphatase) substrate

1. 12.1g TRIS + 920ml a.d. + 60ml 1N HCl
2. 0.2g Naphthol-AS MX-phosphate in 20ml dimethylformamide, add to TRIS
3. Add 1ml 1M Levamisole
4. Mix well and aliquot 50ml in Falcon tubes
5. Store at -20°C

Working solution
50ml (1 Falcon tube)
0.05g Fast Red TR salt
→ Filter it

Appendix B:

Buffers & solutions

Xylene (J.T. Baker)

Ethanol (EtOH) at concentrations 96%, 70%, and 50%

Mayer's Hemalaun (Merck)

Eukitt (Sigma)

Methanol/H2O2 (0.2% H2O2)
150 ml methanol
1 ml 30% H2O2

HCl-Ethanol
0.5 ml 37% HCl (Sigma-Aldrich)
100 ml 70% ethanol

Scott's solution
2 g KHCO3 (Merck)
20 g MgSO4 x 7H2O (Merck)
1 L a.d.

Eosin solution
Eosin stock solution
10 g Eosin
100 ml a.d.
→ Let stand for some days
Eosin working solution
250 ml of 1:100 dilution of eosin stock
12 drops glacial acidic acid

Luxol Fast Blue

1g Luxol Fast Blue in 1000mL 96% ethanol
→ solve over night at 57°C

Periodic acid

4g periodic acid
500ml a.d.

Sulfite washing solution

500ml a.d.
5ml conc.HCl (37%)
20ml 10% potassium- or sodium metabisulfite (in a.d.)

TBS-buffer

TBS-stock solution pH 7,5
151.425g TRIS
450g NaCl
1L 1N HCl
2.5 L a.d.

TBS working solution
Dilute stock solution 1:20
50ml stock
950ml a.d.

PBS

Stock solution (0.2M phosphate buffer "Sörensen" pH 7.4 incl. NaCl)
13.8g NaH2PO4 0.04M
71.2g NA2HPO4 0.16M
90g NaCl
2.5 L a.d.

Working solution

Dilute stock solution 1:4
250ml stock solution
750ml a.d.

Aqueous mounting medium – Geltol

1. 60g Glycerol + 24g Mowiol → stir at least 30min in plastic beaker
2. Add 60ml a.d., incubate it for 2h at room temperature
3. Add 120ml TRIS pH 8.5 buffer
4. Heat the solution up to 50°C, incubate solution at 50°C 10min
5. Fill into falcon tubes
6. Centrifugate 15min at 5000G

0.2M TRIS pH 8.5 buffer
3.635g TRIS
150ml a.d.

Aqueous mounting medium for fluorescence – Gallate/Geltol

10ml Geltol
0.2g Gallate = 0.1M
→ Mix over night at room temperature

CSA

1. Borate Buffer: 0.1545g boric acid (Merck 1.00165) in 50ml dist. water
2. Adjust the pH 8.0 with NaOH
3. 6ml borate buffer + 15mg sulpho-NHS-LCS-biotin (Pierce, P.O.B. 117, Illinois, 61105, USA – No. 21335)
4. Add 4.5 mg Tyramine (Sigma T-7255)
5. Stir overnight at room temperature
6. Filter (0.45 µm)
7. Make small aliquots (10-20 µl), store at –20°C

Appendix C:

List of abbreviations

ADCC Antibody-dependent cellular cytotoxicity

AEC 3-amino-9-ethylcarbazole

AP Alkaline phosphatase

BBB Blood-brain barrier

BCR B cell receptor

BDNF Brain-derived neurotrophic factor

C region Non-antigen-binding constant region of an antibody

CCL2 Chemokine ligand 2

CD Cluster of differentiation

CFA Complete Freund's adjuvant

CHO Chinese hamster ovary cell line

CIH Chromogenic immunohistochemistry

CIS Clinically isolated syndrome

CNS Central nervous system

CSA Catalytic signal amplification

CSF Cerebrospinal fluid

CTL $CD8^+$ cytotoxic T lymphocyte

d12 Day12

d16 Day 16

DAB 3,3'-Diaminobenzidine

DC Dendritic cell

EAE Experimental autoimmune encephalomyelitis

EDTA Ethylenediaminetetraacetic acid

EOMES Eomesodermin

Fab Antigen-binding fragment of an antibody

Fc region Fragment crystallizable region of an antibody

FcR Fragment crystallizable receptor

FCS Fetal calf serum

FcγRIIIα Fcγ receptor IIIα

FFPE Formalin-fixed paraffin-embedded

FUT8 Fucosyltransferase 8

GlcNAc N-acetylglucosamine

GrB Granzyme B

HE Hematoxylin-eosin

HEK Human embryonic kidney 293 cell line

HIER Heat-induced epitope retrieval

HRP Horseradish peroxidase

IFN-γ Interferon γ

Ig Immunoglobulin

IHC Immunohistochemistry

IL Interleukin

iTreg Induced T regulatory cell

LFB-PAS Luxol fast blue-periodic acid schiff

mAb Monoclonal antibody

MAG Myelin-associated glycoprotein

MBP Myelin basic protein

MHC Major histocompatibility complex

mIg Membrane-bound immunoglobulin

MOG Myelin oligodendrocyte glycoprotein

MOGAD Myelin oligodendrocyte glycoprotein antibody-associated disease

MS Multiple sclerosis

NK cell Natural killer cell

NKT cell Natural killer T cell

NMSOD Neuromyelitis optica spectrum disorder

nTreg Natural T regulatory cell

OPC Oligodendrocyte progenitor cells

PAS Periodic acid-schiff

PBS Phosphate-buffered saline

PLP Proteolipid protein

PP Primary progressive

RR Relapse-remitting

SP Secondary progressive

TBS Tris-buffered saline

TCR T cell receptor

Th cell $CD4^+$ T helper lymphocyte

TNF Tumor necrosis factor

Treg T regulatory cell

Tris Tris(hydroxymethyl)aminomethane

YB2/0 YB2/0 cell line – derivative of hybrid myeloma YB2/3HL cell line